UNCLASSIFIED
[redacted]

3 1176 00084 7146

NACA

RESEARCH MEMORANDUM

EFFECTS OF AIRFOIL PROFILE ON THE TWO-DIMENSIONAL FLUTTER DERIVATIVES FOR WINGS OSCILLATING IN PITCH AT HIGH SUBSONIC SPEEDS

By John A. Wyss and James C. Monfort

Ames Aeronautical Laboratory
Moffett Field, Calif.

CLASSIFICATION CHANGED

To UNCLASSIFIED

By authority of NASA TPA 8 Effective Date 9-22-59

NB 9-14-59

LIBRARY COPY

MAY 27 1954

LANGLEY AERONAUTICAL LABORATORY
LIBRARY, NACA
LANGLEY FIELD, VIRGINIA

CLASSIFIED DOCUMENT

This material contains information affecting the National Defense of the United States within the meaning of the espionage laws, Title 18, U.S.C., Secs. 793 and 794, the transmission or revelation of which in any manner to an unauthorized person is prohibited by law.

NATIONAL ADVISORY COMMITTEE
FOR AERONAUTICS
WASHINGTON
May 24, 1954

[redacted]

UNCLASSIFIED

UNCLASSIFIED

[redacted]

NATIONAL ADVISORY COMMITTEE FOR AERONAUTICS

RESEARCH MEMORANDUM

EFFECTS OF AIRFOIL PROFILE ON THE TWO-DIMENSIONAL FLUTTER DERIVATIVES FOR WINGS OSCILLATING IN PITCH AT HIGH SUBSONIC SPEEDS

By John A. Wyss and James C. Monfort

SUMMARY

Aerodynamic lift and moment flutter derivatives were determined at high subsonic speeds for a series of two-dimensional airfoils varying in thickness and thickness distribution. The wings were sinusoidally oscillated about the quarter-chord axis at Mach numbers from about 0.5 to 0.9. The corresponding reduced frequency ranges varied from 0.045 to 0.45 at $M = 0.5$ and from 0.025 to 0.25 at $M = 0.9$. An evaluation of the results indicated that wing profile and angle of attack have major effects on the flutter derivatives at speeds exceeding the Mach number for steady-state lift divergence. In general, at supercritical Mach numbers the trends of the magnitudes of the oscillatory lift coefficients were qualitatively indicated by the trends of the nonoscillatory coefficients, with phase angles, except for the 12-percent-thick airfoil, having only moderate deviation from subsonic theory. The variations in the magnitude of the moment derivative and in its phase angle, resulted in a trend toward instability at supercritical Mach numbers. In particular, for airfoils of equal thickness the effect of an extreme forward location of maximum thickness was destabilizing in that negative aerodynamic damping existed, implying the possibility of a single degree of freedom type of flutter. Decreasing airfoil thickness delayed the large deviation from subsonic theory to higher Mach numbers.

INTRODUCTION

This report is concerned with the evaluation of the effects of airfoil profile on the lift and moment flutter derivatives as measured, by means of pressure cells, on harmonically vibrating two-dimensional wings at high subsonic speeds. It is well-known that theory does not account properly for such factors as flow separation and shock formation, hence, the aircraft designer must of necessity look to experimental values

[redacted]

UNCLASSIFIED

whenever such mixed-flow conditions are encountered. Numerous previous investigations at lower speeds, such as those by Clevenson and Widmayer (ref. 1) and by Halfman (ref. 2), may be cited. With the use of a different measuring technique, the present work extends these previous investigations to higher Mach numbers so that emphasis may be placed upon supercritical speeds for which information is meager or nonexistent.

Since wing profile may be expected to have a significant effect on mixed-flow conditions, several models were used to determine the effects of wing thickness and thickness distribution on the flutter derivatives. NACA 65A series symmetrical airfoils, 12, 8, and 4 percent thick, were used along with two other 8-percent-thick airfoils with their maximum thickness at about 16 and 63 percent of the wing chord. The models were oscillated about the quarter-chord axis at Mach numbers from 0.5 to 0.9 with reduced frequency ranges from 0.045 to 0.45 and from 0.025 to 0.25, respectively. Reynolds numbers, based on the airfoil chord, varied from 5 to 8 million.

SYMBOLS

a	velocity of sound in undisturbed air, ft/sec
b	wing semichord, ft
c_l	dynamic section lift coefficient
c_m	dynamic section moment coefficient about quarter point of chord
f	frequency of oscillation, cps
k	reduced frequency, $\frac{\omega b}{V}$
M	Mach number, $\frac{V}{a}$
M_α	oscillatory aerodynamic section moment on wing about axis of rotation, positive with leading edge up
P_α	oscillatory aerodynamic section lift on wing, positive upwards
q	free-stream dynamic pressure, lb/sq ft
V	free-stream velocity, ft/sec

α oscillatory angular displacement (pitch) about axis of rotation, positive with leading edge up, radians

α_m mean angle of attack about which oscillation takes place, deg

θ phase angle between oscillatory moment and position α, positive for moment leading α, deg

φ phase angle between oscillatory lift and position α, positive for lift leading α, deg

ω circular frequency, $2\pi f$, radians/sec

$\left|\frac{dc_l}{d\alpha}\right|$ magnitude of dynamic lift-curve slope, $\left|\frac{P_\alpha e^{-i\varphi}}{2bq\alpha}\right|$, per radian

$\left|\frac{dc_m}{d\alpha}\right|$ magnitude of dynamic moment-curve slope, $\left|\frac{M_\alpha e^{-i\theta}}{4b^2q\alpha}\right|$, per radian

$\left|\frac{dc_m}{d\alpha}\right|\sin\theta$ aerodynamic damping component in phase with angular velocity

APPARATUS AND METHOD

Models and Instrumentation

The 12- and 8-percent-thick airfoils, NACA 65A012, 65A008, 2-008, and 877A008[1] profiles, were of wood-rib and wood-stressed-skin construction built around steel spars at the quarter chord, which was the axis of rotation. Several wood spars at other chordwise locations were used to minimize spanwise twisting since the models were driven from one side. The 4-percent-thick model, of NACA 65A004 profile, was machined from solid aluminum with a parting line in the chord plane. The upper and lower halves of this model were bolted and doweled together. Each model had a chord of 24 inches and a span of 18-1/4 inches. The gaps between the ends of the models and tunnel walls were sealed with sliding spring-loaded felt pads or brass strips which moved with the models.

---

[1]An NACA 847A110 airfoil was modified to a symmetrical section by using the lower surface coordinates for both upper and lower surfaces and then reducing the thickness ratio to 8 percent.

In figure 1, the model profiles are illustrated to show the variation of thickness and thickness distribution. The reference model, NACA 65A008, is marked to indicate the locations of the pressure cells. Model instrumentation consisted of 15 flush-type pressure cells (see refs. 3 and 4) and 15 pressure orifices along the midspan of each surface of each model. The pressure orifices adjacent to each pressure cell were used for two purposes: (1) as a means to determine the time-average chordwise pressure distribution with the use of a multiple mercury manometer, and (2) to provide an internal reference pressure for the pressure cells. The tubes from each cell and from the adjacent pressure orifice were interconnected at the manometer. In order that the internal reference pressure of the pressure cells would be essentially steady, about 50 feet of 1/16-inch tubing was used from the orifice to the manometer and back to the pressure cell.

Two 14-channel oscillographs were used to record the instantaneous electrical difference of the output of each pair of cells (proportional to the pressure difference between the upper and lower surface at each chord station) and to record the summation of all cells (proportional to the variation of the lift force). The output of an NACA slide-wire position transducer, proportional to the model angle of attack, was simultaneously recorded.

Tunnel, Model Drive System, and Tests

The models were oscillated in the two-dimensional test section in the Ames 16-foot high-speed wind tunnel (ref. 5). The two-dimensional channel was about 20 feet long and 16 feet high. A view of a model in place and a diagrammatic sketch of the drive system are presented in figure 2. The drive rods and sector arm attached to the model were contained within one of the channel walls.

Records were obtained with Mach number and mean angle of attack constant for frequencies from 4 to 40 cycles per second at intervals of 4 cycles per second and for an amplitude of $\pm 1^\circ$. Data are presented for mean angles of attack of 0° and 2° and for Mach numbers from 0.5 to about 0.9. Sample oscillograph records which illustrate the necessity for harmonic analysis at the higher Mach numbers are given in figure 3. The lift was evaluated by a 12-point harmonic analysis of three consecutive cycles of the sum trace. The pitching moment was evaluated by a 12-point harmonic analysis of the individual cell traces for one cycle.

Since the investigation was conducted in a closed-throat tunnel, the effects of wind-tunnel resonance must be accounted for either by avoiding conditions in which tunnel-wall effects are significant or by correcting the results for the effects of the tunnel walls (refs. 6 and 7). Calculations made at the Langley and Ames Laboratories employing

the single-doublet-line, single-control-point solution described in reference 7 yielded the following results for a tunnel height of 16 feet, wing chord of 2 feet, and Mach number of 0.7: At frequencies of 10, 20, and 40.66 cycles per second, the magnitudes of the coefficients were increased by 3.8, 5.0, and 4.7 percent, respectively, due to the presence of the tunnel walls. These results indicate that, for the conditions of the calculations, the effect of the tunnel walls was small. However, for mixed-flow conditions, the application of such corrections based on potential flow would be questionable; hence, to minimize tunnel-wall effects, all data obtained at frequencies within 10 percent of the tunnel resonant frequency (refs. 6 and 7) have been omitted. Although the use of such a procedure does not mean tunnel-wall effects have been completely eliminated over the entire frequency range, it is felt that tunnel-wall effects are not a predominant factor in the trends of the data.

For a discussion of other factors influencing the precision of the data, the reader is referred to references 3 and 4.

RESULTS AND DISCUSSION

A tabulation of the measured derivatives is contained in tables I, II, III, IV, and V for the NACA 65A012, 65A008, 65A004, 2-008, and 877A008 airfoils, respectively. The results concerning lift derivatives are first discussed and are presented in figures 4 to 10, followed by a discussion and the presentation of the moment derivatives in figures 11 to 15.

Lift

Experimental values for the reference model for three representative Mach numbers are presented in figure 4 as a function of reduced frequency. In this figure, as in subsequent figures, the absolute magnitude of the flutter derivative is expressed in terms of the slope of the lift curve per radian and the corresponding phase-angle relationship between the lift vector and model angle of attack in degrees. Theoretical values at Mach numbers of 0.5, 0.6, and 0.7 may be obtained from the work of Dietze (refs. 8 and 9), and at Mach numbers of 0.8 and 1.0 from Minhinnick (ref. 10) and Nelson and Berman (ref. 11), respectively.

In this figure it may be noted that at 0.49 and 0.79 Mach numbers the flutter derivatives tend to increase with increasing reduced frequency; furthermore, there seems to be a large variation in the phase angle at low values of reduced frequency at 0.79 Mach number. However,

Mach number appears to have had a greater effect on the data than did frequency at 0.91 Mach number.

Typical results as a function of Mach number are presented in figure 5 for the reference model, the NACA 65A008 airfoil. The lines showing the theoretical values are identified at one end by the frequency in cycles per second to which they pertain. Since theoretical values have been computed in the cited references only at certain Mach numbers which have already been indicated, an interpolation was necessary to obtain values at intermediate Mach numbers. Although such an interpolation inherently involves some error, a consistent set of values was nevertheless established and was used for the purpose of determining the effects of varying airfoil shape.

To distinguish between the various frequencies, the experimental and theoretical values are each faired with the same type of line. For example, the experimental and theoretical values for a frequency of 8 cycles per second are each shown with a solid line. Examination of the experimental data for a frequency of 8 cycles per second indicates that the trends of both experiment and theory were the same at low Mach numbers. As Mach number increased, a large decrease in the magnitude of the experimental derivative occurred, accompanied by a variation of phase angle such that the trend toward increasing lag was reversed. Although the agreement with theory was not precise at the lower Mach numbers, it may be seen that the general trends for all frequencies were nearly the same.

The data from figure 5 are presented in a different form in figure 6; the experimental magnitude has been divided by the theoretical magnitude, and the theoretical phase angle has been subtracted from the experimental phase angle. These quantities are also shown as a function of Mach number. If the experimental and theoretical values exactly agreed, the ratio of the magnitudes of the derivatives would be 1, while the difference in phase angle would be 0. The faired lines represent the average deviation from theory for the entire frequency range up to 40 cycles per second.

It is of interest to note that the individual points do not indicate an entirely random scatter about the mean line for the various frequencies. For example, examination of the points for 40 cycles per second in the top portion of the figure shows that these points are usually the uppermost value at each Mach number. Hence, this figure not only provides some indication of the range of the experimental values, but illustrates the fact that, although the values depend on frequency, the general variations with Mach number are represented by the faired average curves.

The use of the average deviation from theory appears to be justified since it is representative of each model. For example, in figure 6 it may be noted that all the experimental points lie within a comparatively

narrow band along the faired curves with the exception of the higher frequencies in the upper portion of the figure. In fact, a band of width ±0.15 in the upper portion of the figure and a band of width ±10° in the lower portion of the figure would contain about 80 percent of all the experimental points. These results are typical of all the models. It might be noted that the averaging process used has the effect of removing frequency as a parameter. It should be noted that each model was oscillated at the same amplitude and through the same range of frequencies, hence the average deviation from theory indicates the over-all effects of airfoil shape and the general trends of the data.

Effect of thickness distribution.- The effects of the variation of thickness distribution as indicated by the curves showing the average deviation from theory over the frequency range tested are summarized in figure 7 for mean angles of attack of 0° and 2°. It would appear from this figure that the main effect of the chordwise location of maximum thickness was on the magnitudes of the derivatives rather than on phase angles, although no systematic trend is apparent.

Effect of wing thickness.- The results showing the effects of wing thickness are presented in figure 8. At an angle of attack of 0°, wing thickness appears to have had a much more pronounced effect than wing-thickness distribution (fig. 8(a) as compared to fig. 7(a)). As might be expected, the primary effect of reducing wing thickness was to delay any large deviation from theory to a higher Mach number.

At an angle of attack of 2° (fig. 8(b)), large differences over the entire range of Mach numbers occurred between the models in the magnitudes of the derivatives.

Comparison with steady-state results.- In order to examine whether any relation existed between unsteady and steady-state results, a comparison with steady-state results obtained from the time-average chordwise pressure distributions for mean angles of attack of 0° and 2° is made in figures 9 and 10. In these figures, the steady-state data have been normalized with the Prandtl-Glauert value of the theoretical lift-curve slope. It may be recalled that the Prandtl-Glauert curve is also obtained as an end condition as the frequency of oscillation approaches zero.

Examination of these figures indicates that although there appears to be some parallelism or similarity between the steady and unsteady curves, the comparison between the steady and unsteady values is at best only qualitative. For example, in neither figure 9 nor figure 10 do the unsteady and steady-state curves coincide throughout the entire range of Mach numbers. It should also be noted that, with the exception of the NACA 65A012 airfoil at a mean angle of attack of 2° (fig. 10(b)), the unsteady values approached theory more closely than did the steady-state

values, particularly at the lower Mach numbers, that is, from $M = 0.5$ to 0.7. Although the effect of the higher frequencies in increasing the level of the curves for the unsteady case may in part account for the differences between the curves, this effect is small. However, the one characteristic that is common to both the unsteady and steady curves in almost every case is a trend toward a reduction in magnitude at the highest Mach numbers. The Mach number at which this trend initiates cannot be precisely delimited, nevertheless, for the three NACA 65A-series airfoils at a mean angle of attack of 0° (fig. 10(a)), the unsteady lift trend appears to be associated with the steady-state flow changes which occur above the Mach number for lift divergence.

It would therefore appear that as a first approximation the Mach number for lift divergence may be taken as a criterion for the onset of significant changes in the trends of the unsteady values, and that this trend toward a decrease in the magnitude of the unsteady values is related to the trend of the steady-state data. It should be pointed out that this conclusion is not as evident for the NACA 2-008 and 877A008 airfoils (fig. 9) and for the NACA 65A004 airfoil at a mean angle of attack of 2° (fig. 10(b)), since these figures indicate that the correlation between the Mach number for lift divergence and the initiation of a downward trend of the unsteady values is not precise and they may differ by as much as 0.1. However, it is felt that there is sufficient evidence presented in figures 9 and 10 to indicate that steady-state values may prove useful as a qualitative indication of the trends of the unsteady-state coefficients at supercritical Mach numbers.

For the steady-state condition the phase angle is, of course, zero; therefore no corollary for the phase angle with relation to the oscillatory condition is possible. However, except for the 12-percent-thick wing, the phase angle shows only a moderate deviation from theory throughout the speed range of the present investigation.

Moment

The moment derivatives for the reference model as a function of reduced frequency for several Mach numbers are presented in figure 11 and as a function of Mach number in figure 12. A comparison of these figures indicates that even though there may have been a greater effect due to frequency on the moment derivatives than had been the case for the lift derivatives, from figure 12 it appears that the effects of Mach number are similar for all frequencies. Hence, the effects of airfoil profile are again compared on the basis of the faired average curves in figure 12 which represent the average deviation from theory over the entire frequency range.

In contrast to the lift results previously presented in figure 6, the magnitudes of the moment derivatives greatly exceeded the theoretical values, along with a much larger variation of phase angle as compared with theory. These results may be attributed to the fact that the comparison is between very small quantities in regard to the magnitude of the derivatives, since the moment is taken about the quarter-chord axis, and to small movements of the center of pressure which would be reflected in large changes of phase angle. The general trends of the results, nevertheless, are represented by the faired average curves.

Effect of thickness distribution.- The effects of the variation of the chordwise location of maximum thickness are shown in figure 13. An apparent characteristic of the NACA 2-008 airfoil, with a forward location of maximum thickness, is a large shift toward a lagging phase angle as Mach number increased above 0.8, such that the phase angle lagged theory by 80° and 90° at angles of attack of 0° and 2°, respectively. The effects of such large shifts in phase angle are discussed in relation to subsequent figures.

Effect of wing thickness.- The effects of wing thickness on the moment derivatives are shown in figure 14. As might be expected, the primary effect of decreasing wing thickness was again to delay any large variations to a higher Mach number.

Instability.- Since there was such a large variation at the higher Mach numbers from the subsonic theoretical values, it is of basic importance to examine the damping-moment derivatives directly to determine whether instability, or the existence of negative aerodynamic damping (implying the possibility of a single degree of freedom type of flutter), which is not predicted by the theory, existed at these speeds. The average damping-moment derivatives for the entire frequency range are therefore presented in figure 15. Also included in this figure are dashed lines indicating average values derived from theory for the corresponding frequency range.

The effect of wing-thickness distribution on aerodynamic damping is shown in figure 15(a) for each mean angle of attack. It may be noted that there was a trend toward instability for each model, with the NACA 2-008 airfoil becoming abruptly unstable at about 0.85 Mach number at 0° and 2° angles of attack. It would appear that stability about the quarter-chord axis increased as maximum thickness was moved toward the trailing edge.

The effect of wing thickness on the aerodynamic damping moment is shown in figure 15(b) for each angle of attack. Although the trend toward instability does not appear at 0° angle of attack for the NACA 65A004 profile, the susceptibility of the thinner wing to negative aerodynamic damping is clearly indicated at the 2° mean angle of attack.

CONCLUSIONS

Within the limitations of speed range and angle-of-attack variation of the investigation, the following general conclusions may be drawn:

1. Section profile has a major effect on the flutter derivatives at speeds exceeding the Mach number for steady-state lift divergence.

2. It appears that the variation in angle of attack has an effect as important as the effect of the variation in profile.

3. In general, at supercritical Mach numbers, a qualitative evaluation of the results indicated that the trends of the magnitudes of the oscillatory lift coefficients were indicated by the trends of the non-oscillatory lift coefficients, with phase angles, except for the 12-percent-thick model, showing only a moderate deviation from theory.

4. The variations in the magnitude of the moment derivative and in its phase angle, resulted in a trend toward instability at supercritical Mach numbers. In particular, for airfoils of equal thickness the effect of an extreme forward location of maximum thickness was destabilizing in that negative aerodynamic damping existed, implying the possibility of a single degree of freedom type of flutter.

Ames Aeronautical Laboratory
National Advisory Committee for Aeronautics
Moffett Field, Calif., Mar. 24, 1954

REFERENCES

1. Clevenson, S. A., and Widmayer, E., Jr.: Preliminary Experiments on Forces and Moments of an Oscillating Wing at High-Subsonic Speeds. NACA RM L9K28a, 1950.

2. Halfman, Robert L.: Experimental Aerodynamic Derivatives of a Sinusoidally Oscillating Airfoil in Two-Dimensional Flow. NACA Rep. 1108, 1952.

3. Erickson, Albert L., and Robinson, Robert C.: Some Preliminary Results in the Determination of Aerodynamic Derivatives of Control Surfaces in the Transonic Speed Range by Means of a Flush-Type Electrical Pressure Cell. NACA RM A8H03, 1948.

4. Wyss, John A., and Sorenson, Robert M.: An Investigation of the Control-Surface Flutter Derivatives of an NACA 65_1-213 Airfoil in the Ames 16-Foot High-Speed Wind Tunnel. NACA RM A51J10, 1951.

5. Sorenson, Robert M., Wyss, John A., and Kyle, James C.: Preliminary Investigation of the Pressure Fluctuations in the Wakes of Two-Dimensional Wings at Low Angles of Attack. NACA RM A51G10, 1951.

6. Runyan, Harry L., and Watkins, Charles E.: Considerations on the Effect of Wind-Tunnel Walls on Oscillating Air Forces for Two-Dimensional Subsonic Compressible Flow. NACA TN 2552, 1951.

7. Runyan, Harry L., Woolston, Donald S., and Rainey, A. Gerald: A Theoretical and Experimental Study of Wind-Tunnel-Wall Effects on Oscillating Air Forces for Two-Dimensional Subsonic Compressible Flow. NACA RM L52I17a, 1953.

8. Dietze, F.: The Air Forces of the Harmonically Vibrating Wing in Compressible Medium at Subsonic Velocity (Plane Problem). AAF, Air Mat. Com., Wright Field, Tech. Intelligence. Trans. F-TS-506-RE, Nov. 1946.

9. Dietze, F.: The Air Forces of the Harmonically Vibrating Wing in a Compressible Medium at Subsonic Velocity (Plane Problem). Part II. AAF Air Mat. Com., Wright Field, Tech. Intelligence. Trans. F-TS-948-RE, Mar. 1947.

10. Minhinnick, I. T.: Subsonic Aerodynamic Flutter Derivatives for Wings and Control Surfaces (Compressible and Incompressible Flow). British R.A.E. Rep. No. Structures 87, July 1950.

11. Nelson, Herbert C., and Berman, Julian H.: Calculations on the Forces and Moments for an Oscillating Wing-Aileron Combination in Two-Dimensional Potential Flow at Sonic Speed. NACA TN 2590, 1952.

TABLE I.- MEASURED FLUTTER DERIVATIVES FOR THE NACA 65A012 AIRFOIL

$\alpha_m = 0^\circ$

M	k	ω	$\left\lvert\frac{dc_l}{d\alpha}\right\rvert$	φ	$\left\lvert\frac{dc_m}{d\alpha}\right\rvert$	θ
0.491	0.103	57.0	6.394	351.8	- - -	- - -
	.184	101.8	5.466	358.8	- - -	- - -
	.282	155.9	5.099	355.5	- - -	- - -
.590	.077	51.6	7.083	351.7	- - -	- - -
	.152	101.3	6.056	351.9	- - -	- - -
	.229	153.2	5.319	351.2	- - -	- - -
.633	.074	52.6	5.745	355.0	0.531	342.1
	.111	79.2	5.068	355.5	- - -	- - -
	.144	103.0	5.299	355.5	.590	317.6
	.183	130.9	4.661	357.3	- - -	- - -
	.218	155.9	4.449	358.0	.585	305.0
	.252	180.0	4.036	349.6	- - -	- - -
	.320	228.5	3.913	15.0	- - -	- - -
	.359	256.5	4.259	16.0	1.008	311.6
.682	.064	49.8	7.918	344.4	.595	325.4
	.097	76.0	7.332	339.7	- - -	- - -
	.130	101.6	6.855	348.2	.658	310.6
	.163	127.3	5.533	337.3	- - -	- - -
	.197	153.7	5.765	346.4	.745	279.7
	.264	206.2	4.362	2.5	.554	291.5
	.293	229.3	5.118	0.8	- - -	- - -
	.325	254.4	4.932	0.4	.868	278.8
.731	.062	51.2	8.080	348.1	.634	326.9
	.098	81.2	8.454	339.5	- - -	- - -
	.121	100.6	7.092	339.5	.675	304.6
	.156	129.4	6.092	328.9	- - -	- - -
	.247	205.6	5.187	356.2	.647	283.0
	.280	232.7	5.299	355.2	- - -	- - -
	.308	256.1	5.018	4.4	.982	279.5
.790	.057	52.2	8.576	343.5	.242	305.4
	.086	77.8	8.362	337.9	- - -	- - -
	.114	103.9	7.476	336.4	.045	276.3
	.142	129.3	6.137	327.1	- - -	- - -
	.199	180.9	4.771	351.7	- - -	- - -
	.226	205.3	4.588	348.9	.464	263.1
	.256	232.7	5.285	356.6	- - -	- - -
.837	.052	50.8	4.894	354.0	.612	301.6
	.077	74.7	4.590	342.7	- - -	- - -
	.104	101.5	4.780	351.6	.828	269.9
	.182	177.3	3.515	2.6	- - -	- - -
	.207	200.9	3.597	12.2	.857	256.9
	.235	228.4	4.444	16.5	- - -	- - -
	.262	255.4	5.123	359.9	1.736	222.0
.885	.030	30.7	.965	47.0	2.719	348.1
	.049	50.3	.641	92.7	3.117	348.0
	.080	82.1	1.725	59.9	- - -	- - -
	.097	99.7	1.884	47.4	2.436	311.4
	.149	153.2	2.681	41.2	1.939	314.4
	.176	181.3	2.015	29.0	- - -	- - -
	.201	207.3	1.454	33.2	1.223	304.0
	.223	230.4	2.733	32.1	- - -	- - -
	.246	253.3	2.681	2.4	1.867	300.0

$\alpha_m = 2^\circ$

M	k	ω	$\left\lvert\frac{dc_l}{d\alpha}\right\rvert$	φ	$\left\lvert\frac{dc_m}{d\alpha}\right\rvert$	θ
0.491	0.058	31.7	6.520	354.6	- - -	- - -
	.094	51.1	5.578	354.1	- - -	- - -
	.136	74.1	5.574	0.0	- - -	- - -
	.187	102.5	4.989	5.3	- - -	- - -
	.238	130.1	4.987	4.5	- - -	- - -
	.287	157.1	5.341	0.0	- - -	- - -
	.328	179.5	5.058	12.4	- - -	- - -
	.469	256.5	4.823	29.4	- - -	- - -
.590	.048	31.5	6.523	352.4	0.559	341.7
	.076	50.5	6.262	345.5	- - -	- - -
	.120	79.4	5.925	347.7	- - -	- - -
	.152	100.8	5.965	354.2	.771	317.8
	.198	131.2	5.488	352.5	- - -	- - -
	.233	154.0	5.213	347.7	.739	297.5
	.347	229.3	4.744	9.2	- - -	- - -
	.384	254.4	5.426	16.1	1.153	304.0
.682	.044	34.6	6.216	354.5	- - -	- - -
	.066	52.0	5.833	349.2	- - -	- - -
	.101	80.2	5.506	347.3	- - -	- - -
	.131	103.7	5.224	0.4	- - -	- - -
	.163	128.9	5.055	348.8	- - -	- - -
	.196	154.8	4.528	342.7	- - -	- - -
	.294	232.7	4.290	15.3	- - -	- - -
	.321	253.7	4.329	2.0	- - -	- - -
.731	.041	34.6	6.788	351.2	.698	340.5
	.060	51.2	6.050	348.9	.642	333.2
	.093	79.2	5.566	349.8	- - -	- - -
	.122	104.5	5.437	351.9	.721	315.6
	.153	130.4	5.280	346.3	- - -	- - -
	.240	204.9	4.182	359.8	.762	300.4
	.271	231.3	4.375	0.6	- - -	- - -
	.299	255.4	4.282	358.2	1.084	292.6
.790	.034	30.9	6.377	353.8	.597	340.3
	.056	50.8	5.981	347.9	.606	316.4
	.086	77.6	7.353	343.3	- - -	- - -
	.115	103.5	6.628	341.9	.688	277.1
	.139	125.1	5.099	333.5	- - -	- - -
	.198	178.5	3.861	353.3	- - -	- - -
	.225	202.7	4.047	348.9	.557	287.3
	.254	228.8	4.196	358.7	- - -	- - -
	.279	251.6	4.895	0.9	1.126	281.6
.837	.031	29.6	4.318	355.4	.285	340.8
	.054	51.8	4.580	357.6	.606	306.3
	.080	77.7	4.775	353.3	- - -	- - -
	.103	100.2	4.570	356.9	.941	281.4
	.181	175.5	3.654	348.1	- - -	- - -
	.208	201.7	4.068	351.4	.675	259.2
	.244	236.5	4.601	13.9	- - -	- - -
	.261	252.3	5.379	5.1	1.316	242.9
.885	.030	30.7	3.497	347.1	1.256	356.8
	.049	50.3	2.751	345.4	.879	350.2
	.080	82.1	3.032	359.2	- - -	- - -
	.097	99.7	2.403	342.9	.712	340.7
	.149	153.2	2.647	353.5	1.389	0.2
	.177	181.3	3.564	351.6	- - -	- - -
	.202	207.3	2.122	336.5	1.043	333.5
	.225	230.4	3.084	345.6	- - -	- - -
	.247	253.3	3.944	356.4	1.364	301.4

NACA

TABLE II.- MEASURED FLUTTER DERIVATIVES FOR THE NACA 65A008 AIRFOIL

$\alpha_m = 0°$

M	k	ω	$\left\lvert\frac{dc_l}{d\alpha}\right\rvert$	φ	$\left\lvert\frac{dc_m}{d\alpha}\right\rvert$	θ
0.491	0.089	48.9	6.186	354.7	- - -	- - -
	.142	78.2	5.638	348.3	- - -	- - -
	.184	101.3	5.507	353.3	- - -	- - -
	.234	128.5	5.319	357.0	- - -	- - -
	.280	153.9	6.250	1.9	- - -	- - -
	.322	177.0	5.518	352.5	- - -	- - -
	.457	251.3	5.883	19.2	- - -	- - -
.590	.074	49.2	6.657	351.0	0.445	315.8
	.116	77.0	5.841	343.6	- - -	- - -
	.152	101.2	5.756	344.9	.626	312.2
	.191	127.2	5.854	347.5	- - -	- - -
	.234	155.9	5.673	349.1	.775	289.8
	.270	179.5	5.500	345.2	- - -	- - -
	.347	231.0	5.612	6.7	- - -	- - -
	.383	254.4	6.787	9.5	1.213	290.0
.680	.065	50.1	6.815	348.9	- - -	- - -
	.102	79.4	6.312	343.0	- - -	- - -
	.130	101.0	6.430	338.4	- - -	- - -
	.167	129.3	6.062	335.7	- - -	- - -
	.199	154.4	5.652	338.2	- - -	- - -
	.295	228.8	6.067	2.0	- - -	- - -
	.329	255.1	6.389	2.3	- - -	- - -
.728	.060	50.4	7.392	340.9	- - -	- - -
	.092	77.2	7.005	339.5	- - -	- - -
	.123	102.5	6.535	335.5	- - -	- - -
	.154	129.1	6.028	331.0	- - -	- - -
	.245	204.9	5.696	347.0	- - -	- - -
	.276	230.4	6.297	348.9	- - -	- - -
	.305	254.9	6.196	352.4	- - -	- - -
.786	.058	52.3	7.999	339.5	.837	323.9
	.086	78.7	7.381	336.1	- - -	- - -
	.114	103.9	6.851	326.9	.805	300.5
	.143	130.2	6.132	320.9	- - -	- - -
	.199	181.4	5.394	348.3	- - -	- - -
	.225	204.9	5.525	344.5	.829	284.5
	.252	229.9	5.800	347.7	- - -	- - -
	.279	254.4	6.848	345.7	1.367	271.4
.833	.050	47.7	7.488	335.9	.454	309.4
	.080	76.1	6.865	332.5	- - -	- - -
	.105	100.7	6.343	325.5	.487	263.8
	.214	204.9	4.705	356.2	.651	291.9
	.238	227.6	5.424	353.5	- - -	- - -
	.263	251.3	6.365	345.7	1.276	272.6
.879	.026	26.7	9.006	336.4	.223	198.6
	.048	49.2	6.862	349.4	.203	281.9
	.074	75.7	7.193	327.6	- - -	- - -
	.149	152.9	4.299	347.6	.093	155.9
	.174	178.8	4.315	353.4	- - -	- - -
	.200	205.6	5.360	358.8	.517	245.9
	.223	229.0	5.990	348.1	- - -	- - -
	.248	255.1	6.383	337.5	1.157	189.3
.917	.029	31.5	3.742	349.8	1.232	327.8
	.048	51.3	3.360	344.3	1.529	319.3
	.073	79.0	2.973	341.9	- - -	- - -
	.118	127.7	3.437	346.7	- - -	- - -
	.145	156.3	3.654	348.4	1.161	300.6
	.167	180.3	3.634	344.9	- - -	- - -
	.188	202.4	3.515	346.1	.922	271.6
	.214	230.5	4.228	349.5	- - -	- - -
	.236	254.3	3.997	341.9	1.440	252.4

$\alpha_m = 2°$

M	k	ω	$\left\lvert\frac{dc_l}{d\alpha}\right\rvert$	φ	$\left\lvert\frac{dc_m}{d\alpha}\right\rvert$	θ
0.492	0.056	30.7	5.356	352.1	- - -	- - -
	.089	48.9	5.074	354.4	- - -	- - -
	.140	76.7	4.613	351.5	- - -	- - -
	.186	101.8	4.571	357.1	- - -	- - -
	.231	126.7	4.205	358.0	- - -	- - -
	.281	154.4	4.510	4.6	- - -	- - -
	.323	177.5	4.443	356.0	- - -	- - -
	.463	254.4	4.828	24.2	- - -	- - -
.590	.031	20.3	6.114	349.6	0.581	341.1
	.076	50.6	5.803	344.2	.557	331.6
	.117	77.8	5.263	346.4	- - -	- - -
	.153	102.0	5.237	348.0	.588	307.1
	.189	125.7	4.883	346.2	- - -	- - -
	.231	153.2	4.975	346.9	.701	284.4
	.271	180.0	4.646	345.5	- - -	- - -
	.346	230.1	4.122	13.9	- - -	- - -
	.378	251.3	5.246	15.7	.964	281.3
.680	.038	29.3	6.618	351.7	.778	341.0
	.066	51.2	6.183	346.8	.806	331.4
	.099	76.3	5.972	343.3	- - -	- - -
	.133	102.6	5.753	341.5	.811	309.7
	.165	127.9	5.641	335.9	- - -	- - -
	.200	154.4	5.339	330.3	.871	282.0
	.296	228.8	5.392	357.5	- - -	- - -
	.327	252.6	5.662	350.6	1.097	278.9
.728	.037	30.7	7.311	350.6	.888	350.5
	.063	52.8	7.347	343.1	.944	330.8
	.095	80.4	6.759	337.6	- - -	- - -
	.127	106.7	6.467	338.7	.972	304.7
	.156	131.3	6.247	326.4	- - -	- - -
	.245	206.2	5.508	349.3	.979	292.6
	.277	233.0	6.156	347.3	- - -	- - -
	.303	255.4	5.911	352.0	1.233	277.5
.761	.036	31.8	8.523	345.2	- - -	- - -
	.059	51.8	7.863	341.9	- - -	- - -
	.091	80.0	6.883	341.2	- - -	- - -
	.117	102.9	6.377	331.2	- - -	- - -
	.146	128.9	6.005	320.8	- - -	- - -
	.206	182.0	4.217	351.8	- - -	- - -
	.234	206.0	5.224	350.2	- - -	- - -
	.261	229.8	5.879	346.7	- - -	- - -
	.290	255.5	6.018	354.4	- - -	- - -
.786	.034	31.1	9.588	347.1	1.086	337.5
	.057	52.5	8.362	337.1	1.092	320.2
	.084	76.7	7.931	333.0	- - -	- - -
	.114	104.1	7.520	326.8	1.053	286.4
	.144	131.6	6.300	318.2	- - -	- - -
	.199	181.8	4.694	349.1	- - -	- - -
	.225	205.8	5.278	340.5	.973	275.8
	.254	232.1	5.627	343.6	- - -	- - -
	.283	258.2	6.853	343.5	1.526	261.3
.833	.030	29.4	8.034	347.4	.487	341.9
	.055	53.5	8.015	338.4	.532	302.9
	.081	79.4	7.464	330.0	- - -	- - -
	.107	104.4	6.595	325.5	.479	254.9
	.160	155.6	4.320	344.1	.206	284.9
	.186	181.1	5.163	348.2	- - -	- - -
	.213	208.3	5.302	355.2	.678	286.3
	.236	230.7	6.237	354.0	- - -	- - -
	.262	256.1	5.502	340.8	1.013	254.1
.879	.031	31.7	7.030	347.9	.380	311.2
	.053	55.2	7.460	331.6	.294	284.4
	.075	77.7	6.721	333.8	- - -	- - -
	.099	103.2	5.835	330.1	.323	198.4
	.150	155.9	4.641	336.5	.197	319.9
	.174	180.7	4.870	351.0	- - -	- - -
	.199	206.5	6.217	348.6	1.062	251.7
	.225	233.5	6.666	344.1	- - -	- - -
	.251	261.1	7.154	337.3	1.175	212.0

NACA

TABLE III.- MEASURED FLUTTER DERIVATIVES FOR THE NACA 65A004 AIRFOIL

$\alpha_m = 0^\circ$

M	k	ω	$\left\lvert\frac{dc_l}{d\alpha}\right\rvert$	φ	$\left\lvert\frac{dc_m}{d\alpha}\right\rvert$	θ
0.594	0.040	27.1	6.212	355.3	0.466	334.7
	.080	53.4	5.849	350.1	.447	320.4
	.109	73.1	5.411	357.0	- - -	- - -
	.149	99.9	5.186	358.3	.517	308.1
	.188	125.7	5.195	8.2	- - -	- - -
	.224	153.3	4.883	353.5	.771	284.8
	.261	178.0	5.242	353.0	- - -	- - -
	.342	233.5	6.989	353.8	- - -	- - -
	.382	260.9	8.995	330.7	1.396	219.8
.691	.035	26.9	6.846	356.1	- - -	- - -
	.064	50.0	6.669	350.8	- - -	- - -
	.097	75.5	6.039	349.9	- - -	- - -
	.131	101.9	5.887	351.2	- - -	- - -
	.162	126.1	5.459	355.9	- - -	- - -
	.194	153.9	5.251	340.4	- - -	- - -
	.258	204.9	4.981	3.0	- - -	- - -
	.294	233.5	7.405	346.9	- - -	- - -
	.327	259.6	7.473	324.3	- - -	- - -
.741	.032	26.6	7.366	354.9	.561	338.2
	.062	54.1	6.996	349.7	.578	327.8
	.089	77.3	6.528	347.5	- - -	- - -
	.117	101.9	6.235	345.9	.629	301.1
	.145	126.5	5.861	339.7	- - -	- - -
	.169	145.3	5.078	329.0	.607	252.3
	.239	205.3	5.599	357.6	.772	272.3
	.269	231.3	7.073	346.5	1.136	285.1
	.303	260.7	7.035	337.8	- - -	- - -
.798	.030	27.4	7.739	354.6	.609	340.3
	.056	50.2	7.522	345.7	.658	320.5
	.083	75.1	7.157	343.9	- - -	- - -
	.115	103.7	6.606	343.5	.705	292.7
	.141	127.6	5.950	335.7	- - -	- - -
	.197	183.7	5.301	343.5	- - -	- - -
	.218	203.0	5.477	343.2	.864	274.3
	.250	233.0	7.536	343.4	1.217	279.4
	.278	259.1	7.924	323.1	- - -	- - -
.850	.026	25.5	9.637	353.9	- - -	- - -
	.053	50.9	8.200	344.4	.664	313.6
	.078	74.8	7.611	340.3	- - -	- - -
	.106	102.2	7.025	337.4	.736	287.1
	.153	153.4	4.590	347.2	.588	276.5
	.179	178.7	4.602	356.0	- - -	- - -
	.208	208.0	5.178	351.7	.928	274.2
	.231	231.4	6.964	298.2	1.611	251.9
	.259	258.5	8.436	325.4	- - -	- - -
.900	.025	25.4	7.315	347.3	.717	331.8
	.050	51.1	8.913	344.6	.738	310.8
	.073	74.1	8.483	337.4	- - -	- - -
	.126	128.2	5.365	329.0	- - -	- - -
	.147	155.4	4.721	341.9	.452	270.6
	.170	180.6	4.819	352.4	- - -	- - -
	.195	206.6	8.097	0.6	1.208	281.8
	.220	232.7	8.076	337.7	1.947	305.2
	.244	258.2	7.635	323.5	- - -	- - -
.942	.025	26.1	5.877	344.2	.438	328.4
	.050	53.2	9.448	335.5	.824	290.3
	.096	102.2	6.885	316.1	.619	298.1
	.120	127.4	4.964	334.7	- - -	- - -

$\alpha_m = 2^\circ$

M	k	ω	$\left\lvert\frac{dc_l}{d\alpha}\right\rvert$	φ	$\left\lvert\frac{dc_m}{d\alpha}\right\rvert$	θ
0.491	0.046	25.5	6.069	357.7	- - -	- - -
	.095	52.5	5.699	2.6	- - -	- - -
	.134	74.0	5.441	5.4	- - -	- - -
	.186	102.5	5.176	8.2	- - -	- - -
	.225	126.9	4.848	8.1	- - -	- - -
	.267	150.3	4.367	12.4	- - -	- - -
	.309	174.0	4.702	2.0	- - -	- - -
	.448	252.3	9.199	341.4	- - -	- - -
.590	.040	26.9	5.862	355.7	0.656	343.0
	.080	53.0	6.011	357.3	.642	334.3
	.112	74.3	5.873	359.8	- - -	- - -
	.154	102.4	5.362	1.2	.859	331.2
	.193	131.4	5.091	351.8	- - -	- - -
	.226	154.0	4.982	351.6	.790	287.4
	.258	176.5	5.501	347.7	- - -	- - -
	.338	231.0	6.340	4.1	- - -	- - -
	.370	252.3	7.528	2.7	1.282	256.7
.691	.033	25.6	7.400	355.6	.808	341.0
	.069	53.2	6.966	351.9	.839	330.2
	.097	74.6	6.718	356.6	- - -	- - -
	.133	102.4	6.316	5.6	.856	332.8
	.164	126.9	6.397	356.4	- - -	- - -
	.192	153.0	6.526	339.5	.984	298.9
	.285	227.1	8.342	350.1	- - -	- - -
	.321	255.8	9.530	330.7	1.564	243.7
.741	.030	25.2	8.117	353.9	.975	345.8
	.059	49.3	7.560	351.7	.970	333.5
	.087	72.5	7.252	353.2	- - -	- - -
	.120	100.0	6.935	358.4	1.004	325.6
	.147	122.7	6.574	359.1	- - -	- - -
	.175	151.6	6.128	332.8	1.034	276.5
	.235	202.7	5.990	354.9	.840	287.3
	.260	224.7	8.895	339.4	- - -	- - -
	.297	256.8	8.784	333.0	1.536	244.6
.798	.029	26.0	9.165	352.9	1.140	344.5
	.059	53.5	9.042	347.4	1.213	327.2
	.083	74.5	8.584	351.7	- - -	- - -
	.114	102.5	7.322	349.1	1.209	318.2
	.135	122.0	6.416	346.1	- ---	- - -
	.191	178.8	6.260	349.0	- - -	- - -
	.218	204.0	7.074	343.7	1.097	280.1
	.244	228.5	9.002	339.2	- - -	- - -
	.275	258.2	10.446	335.9	2.054	257.2
.852	.029	25.6	10.793	348.5	.966	334.7
	.060	52.3	9.672	346.1	1.364	321.2
	.086	75.3	9.016	339.5	- - -	- - -
	.117	103.0	8.075	345.2	1.227	301.6
	.139	121.8	6.564	326.2	- - -	- - -
	.176	177.5	5.269	345.7	- - -	- - -
	.204	205.1	5.928	353.7	1.430	282.7
	.228	230.2	8.365	336.3	- - -	- - -
	.253	254.7	9.206	338.2	2.450	279.5
.870	.026	26.3	11.945	344.7	- - -	- - -
	.049	49.7	11.356	339.1	- - -	- - -
	.074	74.7	9.377	327.6	.405	246.6
	.101	101.7	7.206	322.6	.510	229.7
	.142	151.4	4.826	342.6	.311	341.8
	.164	174.9	5.713	356.1	- - -	- - -
	.190	202.7	6.913	350.5	.908	288.9
	.212	226.4	7.880	340.0	- - -	- - -
	.238	254.7	9.150	331.8	1.546	215.5
.904	.026	27.1	12.237	347.7	1.008	180.1
	.050	52.7	10.817	326.0	1.162	147.2
	.068	72.1	9.216	325.6	- - -	- - -
	.117	123.5	5.181	336.7	- - -	- - -

NACA

TABLE IV.- MEASURED FLUTTER DERIVATIVES FOR THE NACA 2-008 AIRFOIL

$\alpha_m = 0^\circ$

M	k	ω	$\left\lvert \frac{dc_l}{d\alpha} \right\rvert$	φ	$\left\lvert \frac{dc_m}{d\alpha} \right\rvert$	θ
0.590	0.040	26.3	6.460	354.6	0.552	347.9
	.081	53.9	6.082	353.5	.591	327.2
	.113	75.3	5.624	351.4	- - -	- - -
	.155	103.0	5.436	352.3	.620	309.3
	.193	128.7	5.425	351.2	- - -	- - -
	.229	152.5	5.287	351.2	.705	288.4
	.350	232.7	5.001	7.0	- - -	- - -
	.390	259.6	6.210	1.2	.805	263.9
.680	.036	27.9	7.006	351.6	.538	329.3
	.069	53.0	6.433	347.9	.615	329.1
	.098	75.5	6.118	349.0	- - -	- - -
	.134	103.9	5.600	347.1	.613	306.9
	.164	127.2	5.437	346.0	- - -	- - -
	.197	152.4	5.227	343.6	.692	284.1
	.266	206.0	4.627	358.3	.587	275.7
	.299	231.0	5.723	356.1	- - -	- - -
	.329	254.7	5.931	350.6	.995	242.3
.728	.031	25.6	8.587	350.5	.788	349.0
	.063	52.8	6.584	347.4	.720	325.8
	.093	77.6	6.363	341.7	- - -	- - -
	.123	102.6	5.600	344.0	.738	303.9
	.151	126.5	5.194	344.7	- - -	- - -
	.249	208.7	4.738	356.3	.375	248.6
	.279	234.4	5.550	355.4	- - -	- - -
	.308	258.2	5.839	353.2	.940	253.1
.786	.029	26.1	8.206	348.5	.665	338.4
	.056	51.1	7.444	341.7	.578	315.3
	.083	75.5	7.015	336.2	- - -	- - -
	.111	101.7	6.296	335.1	.659	285.2
	.140	127.5	5.053	335.1	- - -	- - -
	.196	178.5	3.884	351.8	- - -	- - -
	.227	206.6	4.799	342.8	.732	256.9
	.253	231.0	5.160	348.3	- - -	- - -
	.280	255.4	6.440	349.1	1.134	246.1
.833	.028	26.8	9.150	344.7	.399	210.5
	.054	52.2	8.806	337.6	.245	218.9
	.080	77.6	7.986	332.1	- - -	- - -
	.108	104.9	6.952	327.3	.357	233.0
	.164	159.9	4.893	338.8	.268	222.6
	.184	179.5	5.420	337.5	- - -	- - -
	.212	206.5	5.576	346.4	.538	227.9
	.239	232.7	6.807	348.3	- - -	- - -
	.263	256.1	7.713	337.3	.525	214.1
.879	.027	27.6	9.720	348.8	1.250	156.3
	.051	53.1	8.316	332.1	1.353	138.2
	.076	78.2	7.062	325.5	- - -	- - -
	.100	103.0	5.235	324.2	.986	139.5
	.150	155.3	3.831	340.4	.454	135.3
	.172	177.5	4.760	342.5	- - -	- - -
	.200	206.0	6.218	341.4	.642	165.4
	.226	233.3	6.432	335.2	- - -	- - -
	.252	259.6	7.107	330.6	1.007	157.7

$\alpha_m = 2^\circ$

M	k	ω	$\left\lvert \frac{dc_l}{d\alpha} \right\rvert$	φ	$\left\lvert \frac{dc_m}{d\alpha} \right\rvert$	θ
0.491	0.052	28.6	6.240	358.2	- - -	- - -
	.093	51.5	5.919	355.0	- - -	- - -
	.137	75.9	5.838	351.4	- - -	- - -
	.181	100.2	5.329	355.5	- - -	- - -
	.228	126.2	5.324	356.2	- - -	- - -
	.278	154.0	5.543	1.2	- - -	- - -
	.327	181.1	5.396	3.1	- - -	- - -
	.465	257.5	5.638	22.5	- - -	- - -
.590	.040	26.8	6.691	354.2	0.574	335.9
	.080	53.9	6.204	346.8	.639	326.9
	.113	75.6	6.093	348.4	- - -	- - -
	.146	98.2	5.706	352.9	.604	297.7
	.193	129.6	5.650	349.6	- - -	- - -
	.231	155.1	5.665	348.5	.737	291.4
	.346	231.9	5.379	4.8	- - -	- - -
	.384	257.5	6.678	1.4	1.042	274.3
.680	.033	25.9	7.347	355.2	.661	335.6
	.069	53.9	6.880	350.0	.676	330.7
	.098	76.2	6.363	347.1	- - -	- - -
	.134	104.1	6.006	349.9	.645	305.5
	.167	130.4	6.026	347.1	- - -	- - -
	.200	155.8	5.475	345.0	.669	277.2
	.299	232.7	5.728	358.5	- - -	- - -
	.331	258.2	6.592	355.5	1.050	274.7
.728	.031	26.0	7.829	358.2	- - -	- - -
	.062	52.5	7.517	354.5	.642	341.4
	.090	75.7	6.957	353.5	- - -	- - -
	.122	103.0	6.932	349.3	.441	301.3
	.152	127.9	6.624	344.6	- - -	- - -
	.245	206.7	6.264	2.6	.599	286.4
	.279	235.6	7.365	358.2	- - -	- - -
	.306	258.2	7.482	358.9	.875	269.5
.786	.029	26.2	8.917	348.2	.086	320.2
	.056	51.8	8.673	344.7	.098	296.0
	.083	76.4	8.193	342.4	- - -	- - -
	.113	104.2	7.768	341.1	.260	253.5
	.140	129.1	6.988	330.8	- - -	- - -
	.227	208.5	5.927	343.6	.405	263.1
	.256	235.6	6.469	344.7	- - -	- - -
	.281	258.2	8.547	347.3	.845	258.1
.833	.028	27.1	9.455	353.9	.317	203.3
	.053	52.4	9.008	345.4	.316	200.2
	.078	76.9	8.618	338.8	- - -	- - -
	.107	104.7	7.950	327.7	.339	172.2
	.185	181.8	5.425	342.0	.346	261.4
	.212	207.6	5.662	349.8	.467	281.4
	.239	234.2	7.075	349.6	- - -	- - -
	.262	257.2	8.568	341.2	1.057	293.6
.879	.027	28.7	10.660	343.1	- - -	- - -
	.052	53.8	8.749	332.4	1.437	142.5
	.075	78.5	6.975	326.0	- - -	- - -
	.100	104.3	5.550	326.9	.527	144.1
	.148	154.2	4.421	335.5	.485	96.8
	.174	181.6	4.481	357.0	- - -	- - -
	.201	209.4	6.225	348.7	.743	179.0
	.225	234.4	6.098	342.3	- - -	- - -
	.248	258.6	6.522	331.1	1.062	166.5

NACA

TABLE V.- MEASURED FLUTTER DERIVATIVES FOR THE NACA 877A008 AIRFOIL

$\alpha_m = 0^\circ$

M	k	ω	$\left\lvert\frac{dc_l}{d\alpha}\right\rvert$	φ	$\left\lvert\frac{dc_m}{d\alpha}\right\rvert$	θ
0.495	0.050	27.9	6.087	352.7	- - -	- - -
	.092	51.5	5.638	349.5	- - -	- - -
	.135	75.7	5.116	347.1	- - -	- - -
	.183	103.0	5.159	348.2	- - -	- - -
	.228	128.2	4.941	355.0	- - -	- - -
	.266	149.6	4.956	350.9	- - -	- - -
	.316	179.5	5.135	338.1	- - -	- - -
	.450	255.4	4.486	4.8	- - -	- - -
.596	.040	27.2	6.246	348.0	0.461	339.8
	.073	49.8	6.243	346.9	.438	324.1
	.109	74.3	5.462	346.5	- - -	- - -
	.153	103.7	5.448	345.2	.609	310.6
	.187	126.9	5.370	345.5	- - -	- - -
	.223	151.7	4.728	346.0	.560	301.9
	.336	231.0	4.267	355.1	- - -	- - -
	.375	257.5	5.053	3.4	.963	293.8
.693	.035	27.5	6.976	348.5	- - -	- - -
	.066	52.2	6.842	343.4	- - -	- - -
	.096	76.7	6.423	343.0	- - -	- - -
	.129	102.5	5.744	341.6	- - -	- - -
	.158	125.8	5.629	339.5	- - -	- - -
	.192	152.7	5.062	336.3	- - -	- - -
	.254	204.4	3.861	0.0	- - -	- - -
	.285	229.9	4.503	356.8	- - -	- - -
	.321	258.9	4.054	356.1	- - -	- - -
.745	.031	26.7	7.230	349.8	.705	336.0
	.060	52.1	6.933	346.6	.664	332.7
	.086	74.1	6.693	341.4	- - -	- - -
	.118	102.0	6.192	341.1	.743	310.8
	.144	124.7	5.863	332.1	- - -	- - -
	.236	206.0	4.294	354.9	.613	312.6
	.262	228.4	4.719	345.5	- - -	- - -
	.291	253.3	4.248	343.6	.906	291.7
.796	.029	26.9	8.056	352.9	.881	345.6
	.056	52.1	7.454	345.6	.599	317.2
	.081	75.5	7.497	337.9	- - -	- - -
	.110	102.2	6.566	334.3	.765	303.4
	.137	127.3	6.077	330.1	- - -	- - -
	.193	180.6	3.642	349.5	- - -	- - -
	.221	207.3	4.442	348.0	.644	317.3
	.250	234.0	4.766	343.6	- - -	- - -
	.280	262.5	5.340	347.5	1.177	289.5
.825	.029	28.2	7.914	348.2	1.168	331.0
	.054	52.1	7.268	348.7	1.113	325.6
	.078	75.6	6.764	340.2	- - -	- - -
	.106	102.7	6.302	331.3	.997	308.1
	.130	125.8	5.291	330.6	- - -	- - -
	.183	178.5	4.023	356.1	- - -	- - -
	.213	207.3	4.605	5.5	1.389	329.1
	.238	231.8	4.581	340.9	- - -	- - -
	.264	257.5	5.601	341.4	1.490	289.5
.857	.027	27.3	6.705	351.3	1.637	349.2
	.051	51.1	6.214	345.8	1.757	338.9
	.074	75.1	6.048	336.9	- - -	- - -
	.103	103.9	5.451	325.8	1.342	320.1
	.152	153.2	3.359	342.3	.722	327.6
	.179	181.6	2.715	338.3	- - -	- - -
	.202	204.9	3.483	331.7	1.518	352.4
	.229	232.2	3.212	333.6	- - -	- - -
	.253	256.5	3.282	334.3	2.161	307.4
.883	.027	27.8	6.494	350.5	1.702	0.6
	.051	53.1	6.162	338.1	1.899	328.1
	.073	76.0	5.577	332.4	- - -	- - -
	.100	104.5	4.493	325.7	1.447	322.8
	.146	152.1	3.493	336.2	1.247	335.1
	.171	179.0	3.023	336.9	- - -	- - -
	.222	232.7	3.928	338.5	- - -	- - -
	.248	259.6	4.504	338.7	1.951	309.5
.910	.116	125.7	3.369	343.7	- - -	- - -
	.135	145.8	3.920	343.3	1.048	162.6
	.166	179.5	4.358	342.5	- - -	- - -
	.197	213.0	4.484	319.9	1.004	174.9
	.213	230.6	4.034	312.8	- - -	- - -
	.240	259.5	3.133	299.7	1.007	173.0

$\alpha_m = 2^\circ$

M	k	ω	$\left\lvert\frac{dc_l}{d\alpha}\right\rvert$	φ	$\left\lvert\frac{dc_m}{d\alpha}\right\rvert$	θ
0.496	0.048	27.1	6.416	353.0	- - -	- - -
	.087	49.1	5.936	350.8	- - -	- - -
	.128	72.1	5.497	351.9	- - -	- - -
	.178	100.0	5.162	349.7	- - -	- - -
	.223	125.4	5.429	347.8	- - -	- - -
	.269	151.4	4.985	344.4	- - -	- - -
	.321	179.5	5.243	351.8	- - -	- - -
	.454	253.3	4.369	18.3	- - -	- - -
.596	.035	24.0	6.579	1.7	0.634	342.4
	.076	51.3	6.457	350.6	.621	333.5
	.108	73.6	5.948	348.7	- - -	- - -
	.147	99.6	5.642	350.8	.765	320.9
	.182	123.9	5.798	352.7	- - -	- - -
	.218	148.2	5.087	347.1	.625	213.6
	.259	174.5	5.325	340.3	- - -	- - -
	.337	227.6	4.688	357.6	- - -	- - -
	.372	251.3	5.319	3.6	1.192	197.6
.693	.031	25.1	6.333	354.2	.536	0.0
	.064	51.3	6.034	352.4	.551	334.7
	.092	73.9	5.614	346.0	- - -	- - -
	.127	101.4	5.562	345.7	.637	310.0
	.153	122.7	5.202	342.1	- - -	- - -
	.187	149.5	4.725	335.9	.659	287.8
	.257	204.2	3.129	4.9	1.487	192.0
	.289	229.3	4.016	0.1	- - -	- - -
	.319	253.3	3.884	358.0	1.044	176.3
.745	.030	26.3	7.318	351.3	.744	352.2
	.058	50.5	7.049	349.0	.819	337.1
	.088	75.8	6.674	343.7	- - -	- - -
	.116	99.8	6.328	342.7	1.006	314.4
	.146	126.0	5.942	337.3	- - -	- - -
	.237	204.0	4.875	355.4	.832	214.5
	.273	235.6	5.120	337.9	- - -	- - -
	.296	255.1	4.560	345.7	.838	210.6
.798	.028	26.1	8.299	354.4	.777	1.5
	.054	50.6	7.410	340.8	.791	322.0
	.079	73.6	7.030	339.8	- - -	- - -
	.109	101.3	6.380	331.4	.804	294.2
	.135	125.7	5.297	322.9	- - -	- - -
	.190	176.5	4.123	335.8	- - -	- - -
	.221	205.3	4.573	345.3	.519	208.7
	.252	233.9	4.611	325.7	- - -	- - -
	.279	259.6	5.128	339.8	.830	228.3
.827	.027	25.9	8.460	346.8	- - -	- - -
	.053	51.5	7.945	344.1	- - -	- - -
	.079	76.1	7.528	334.0	- - -	- - -
	.107	103.4	6.133	330.2	- - -	- - -
	.185	178.5	2.884	345.7	- - -	- - -
	.210	203.3	3.100	2.7	- - -	- - -
	.240	231.8	4.054	347.1	- - -	- - -
	.255	246.4	4.952	348.9	- - -	- - -
.860	.026	26.3	8.294	351.4	.997	355.2
	.051	51.6	7.660	334.9	.761	320.6
	.074	74.3	6.404	324.6	- - -	- - -
	.098	99.2	5.707	315.4	.776	283.4
	.153	154.2	3.976	331.0	.643	298.6
	.178	179.5	4.292	326.1	- - -	- - -
	.204	205.8	4.064	335.9	.770	183.2
	.228	230.4	4.321	323.0	- - -	- - -
	.252	254.7	3.773	317.3	1.606	148.8
.892	.025	26.1	9.005	340.4	.446	0.0
	.049	50.3	7.821	333.4	1.172	209.3
	.073	75.3	6.752	317.0	- - -	- - -
	.147	151.7	3.753	334.9	.520	327.7
	.173	181.6	3.123	329.0	- - -	- - -
	.202	212.2	3.685	332.2	.172	171.7
	.224	235.3	3.168	323.5	- - -	- - -
	.245	257.5	2.675	314.0	.755	322.4

[redacted]

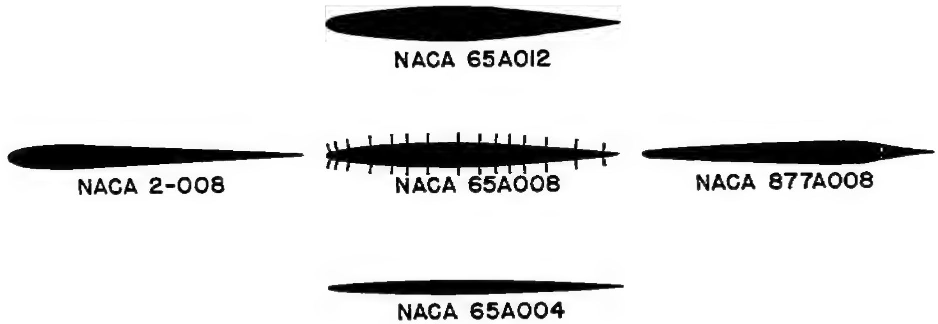

MODEL PRESSURE-CELL LOCATIONS
[In Percent of Model Chord]

Cell number upper and lower surface	65A012 and 65A008	65A004 2-008, and 877A008
1	1.25	1.25
2	3.75	3.75
3	7.5	7.5
4	15	15
5	22.5	22.5
6	27.5	27.5
7	35	35
8	45	45
9	52.5	52.5
10	57.5	57.5
11	62.5	62.5
12	67.5	67.5
13	75	75
14	85	85
15	95	90

Figure 1.- Section profiles and pressure-cell locations of models.

A-14566

(a) Downstream view.

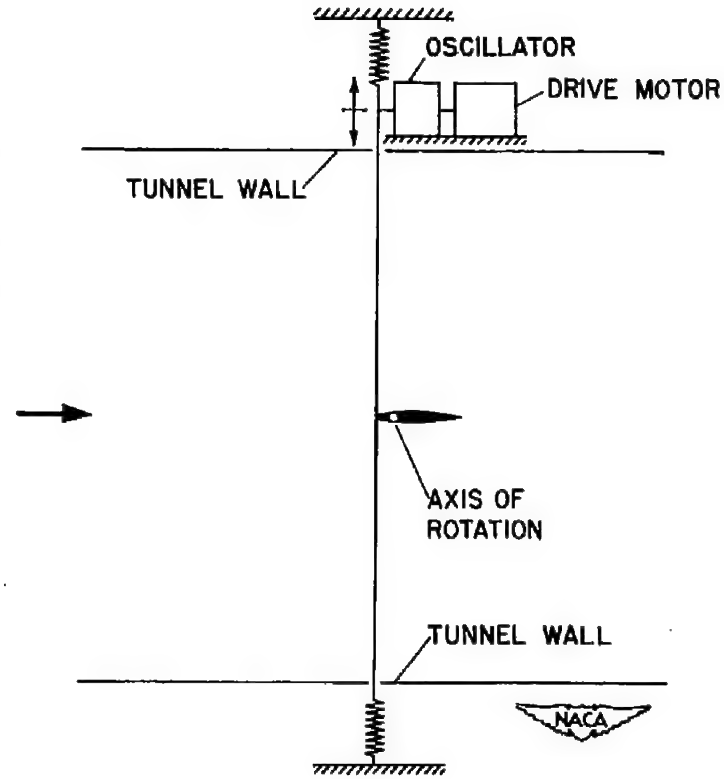

(b) Drive system.

Figure 2.- View of test section with model in place and diagrammatic sketch of drive system.

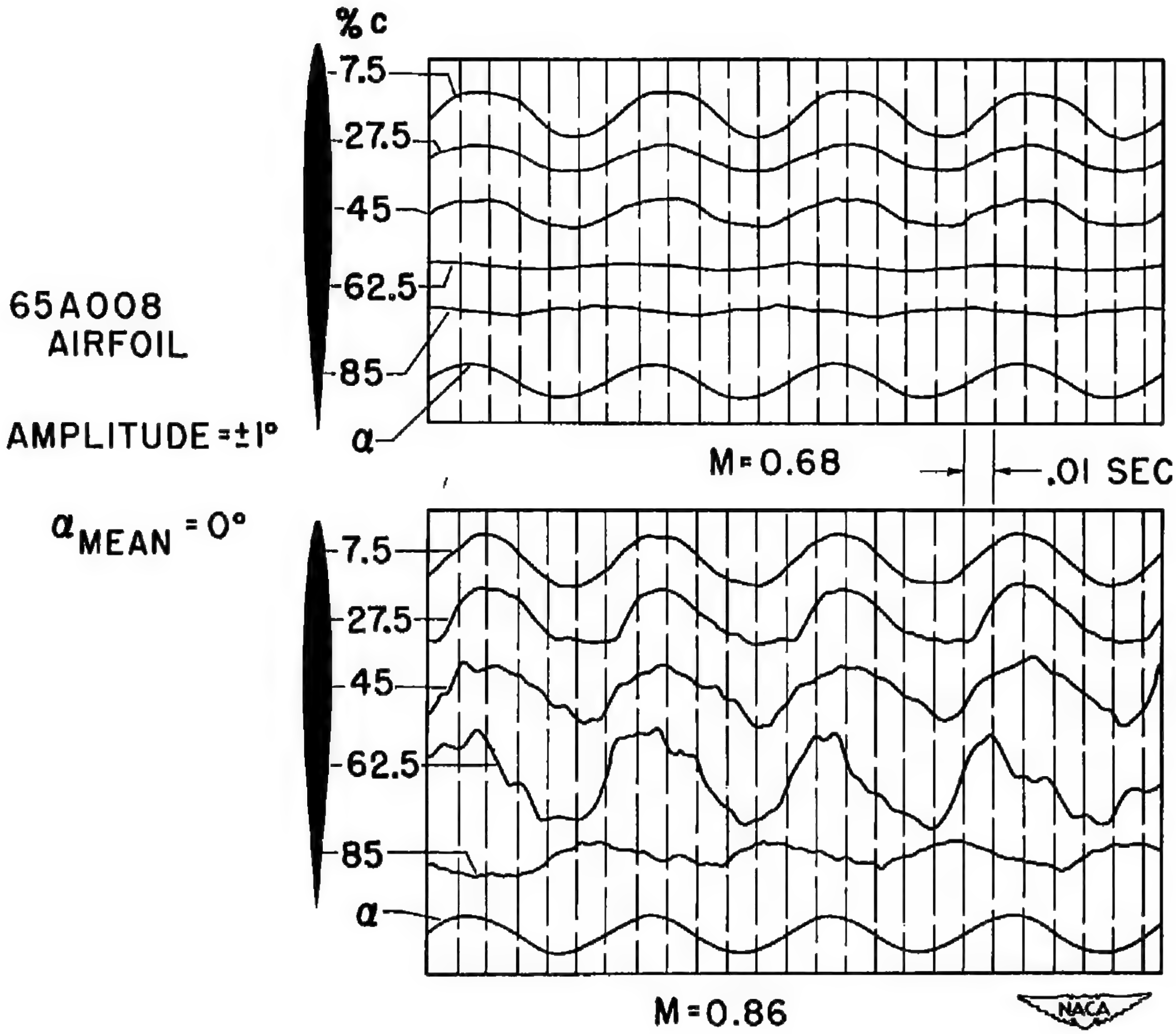

Figure 3.- Typical oscillograph traces.

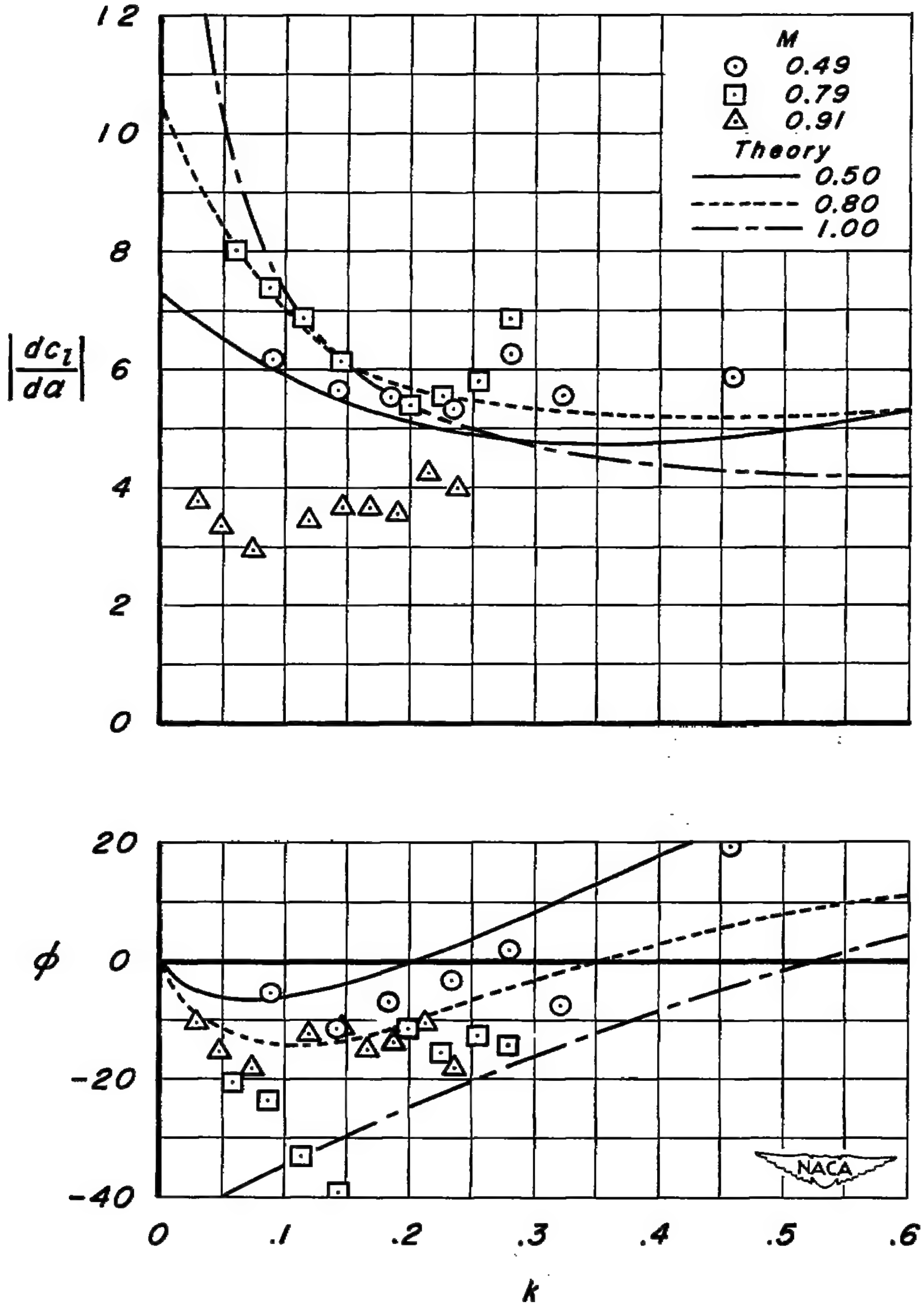

Figure 4.– Results as a function of reduced frequency, k, for several Mach numbers for the reference model, NACA 65A008; $\alpha_m = 0°$.

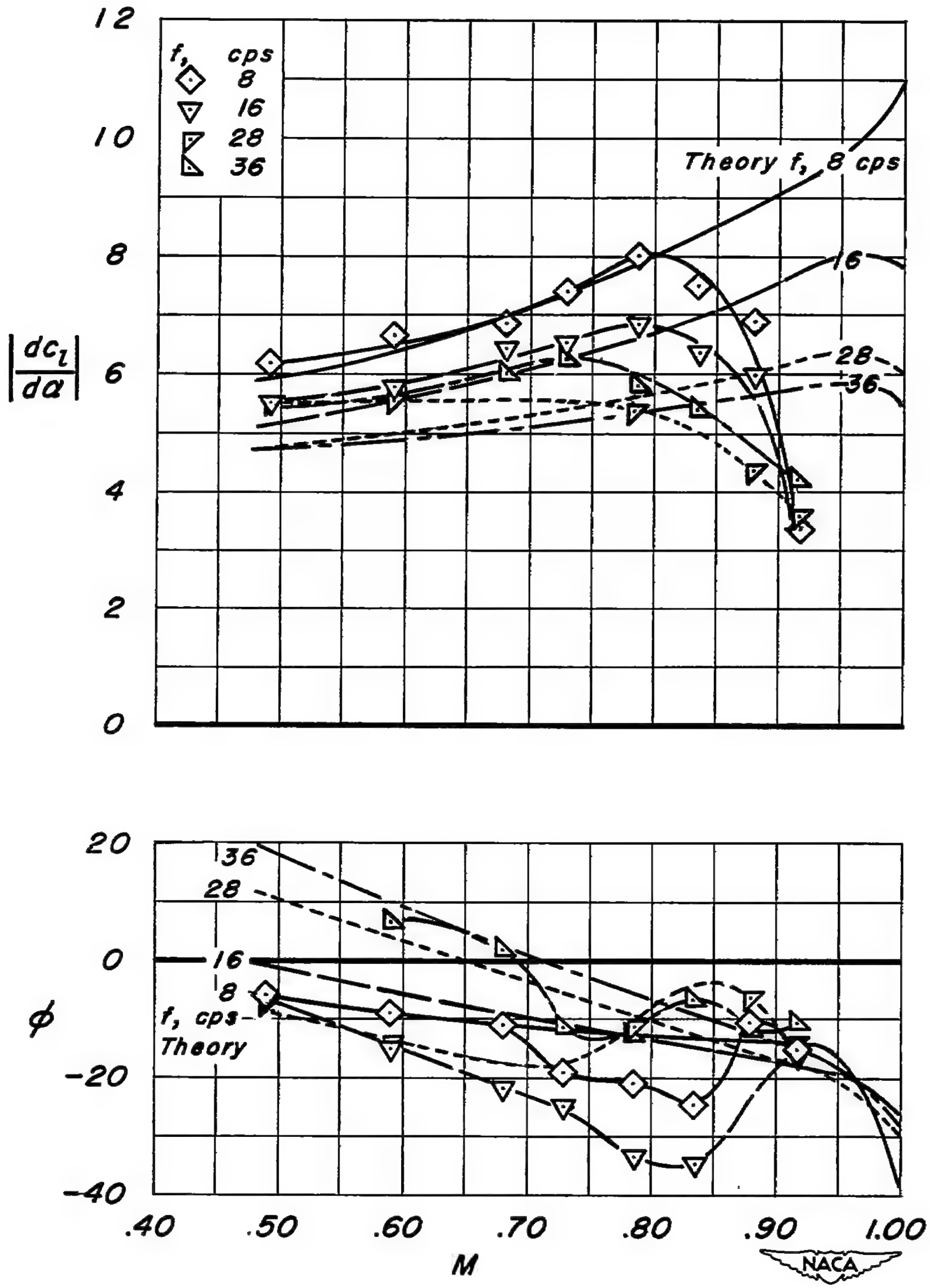

Figure 5.- Typical results for reference model, NACA 65A008; $\alpha_m = 0°$.

[redacted]

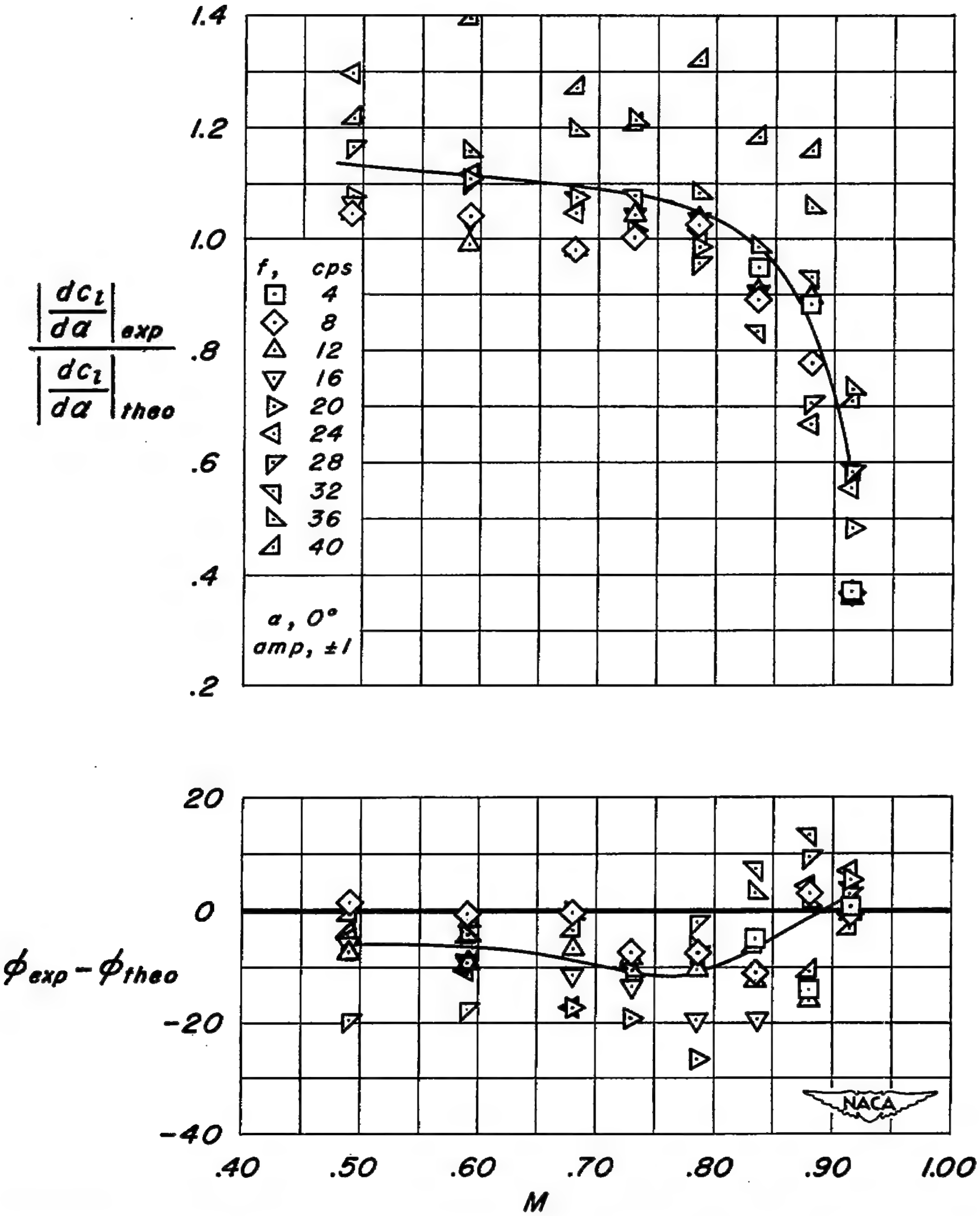

Figure 6.- Variation of experimental results from theory for reference model, NACA 65A008, with a faired line to show the mean variation with Mach number; $\alpha_m = 0°$.

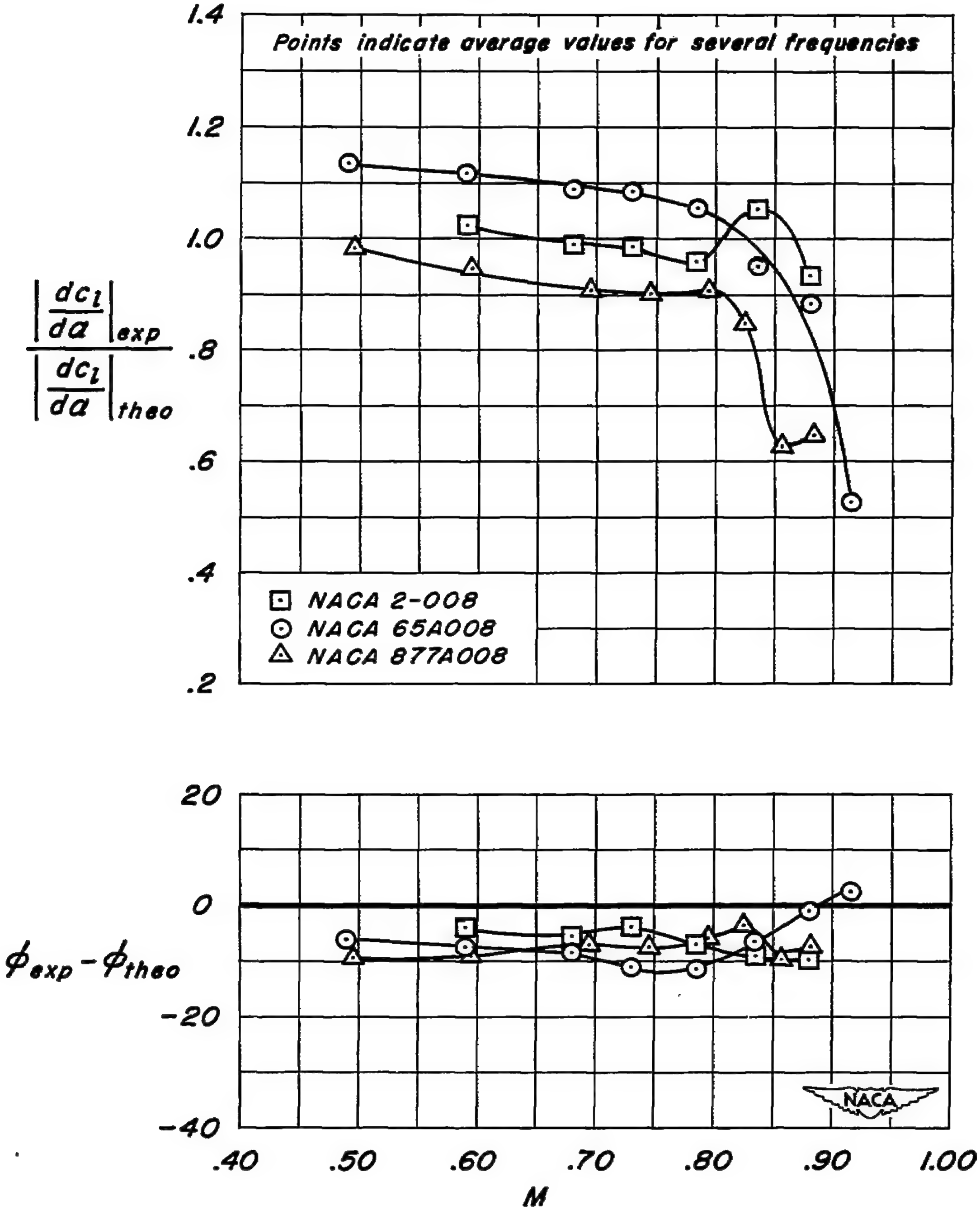

(a) $\alpha_m = 0°$

Figure 7.- Effect of airfoil thickness distribution on lift derivatives.

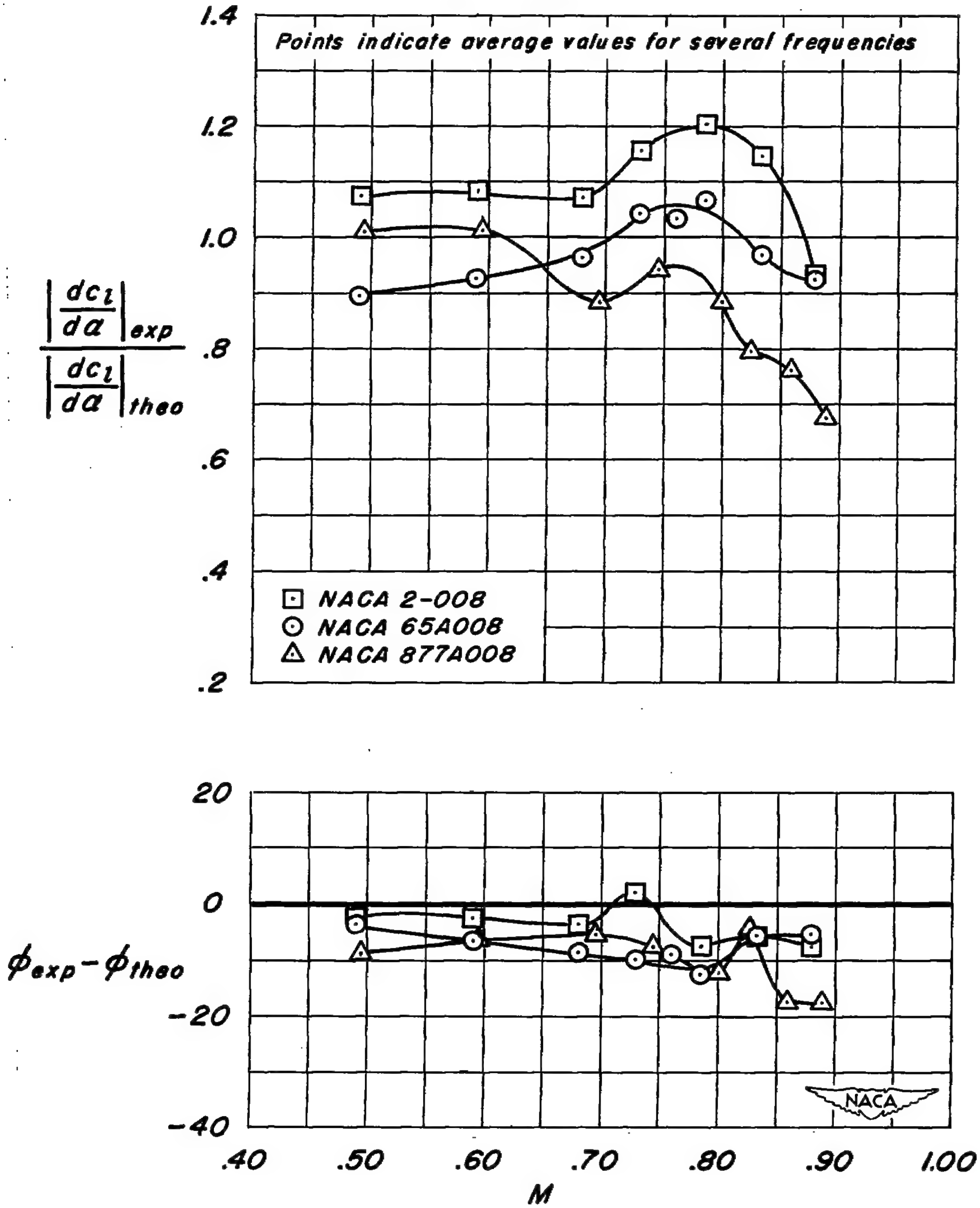

(b) $a_m = 2°$

Figure 7.- Concluded.

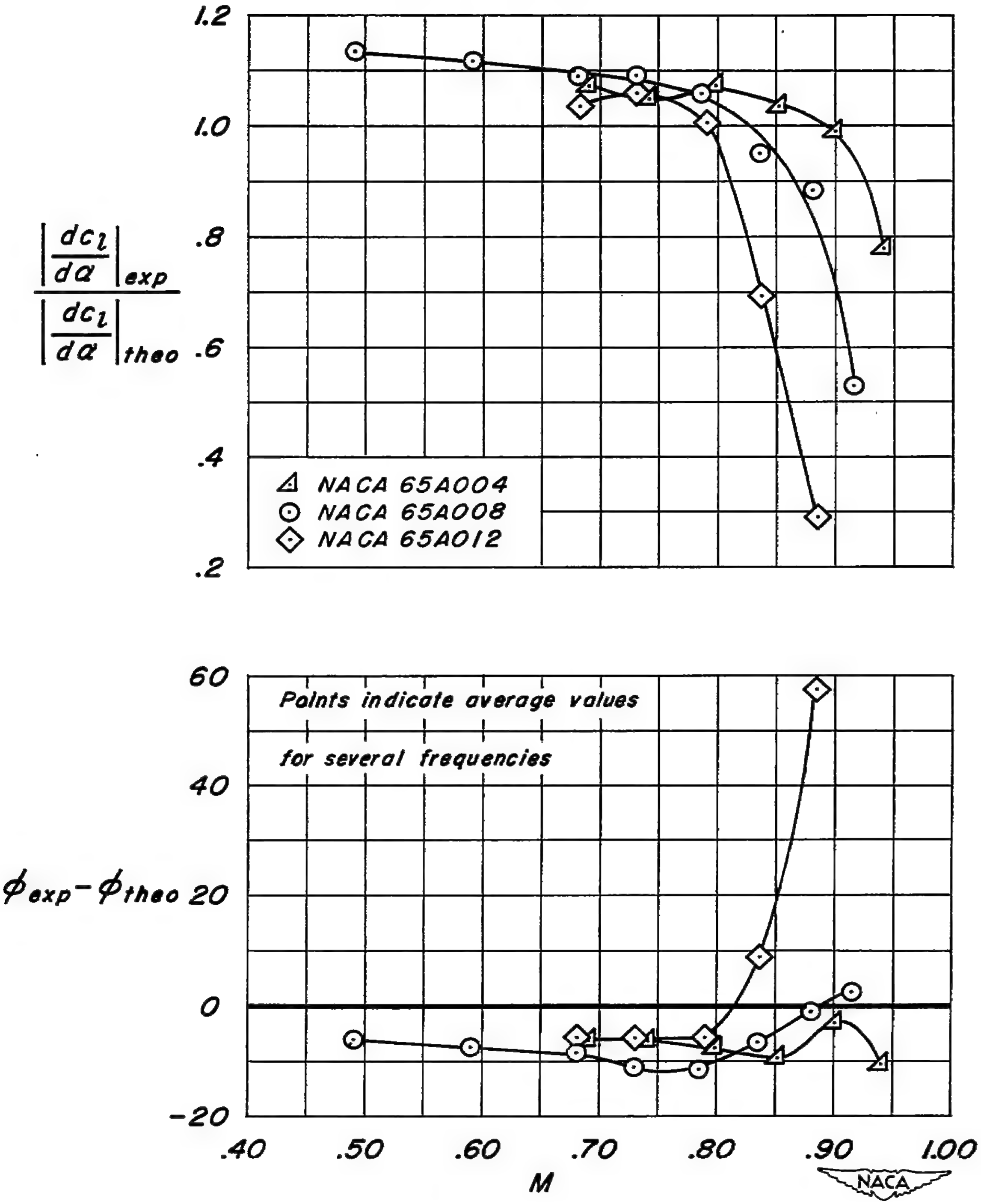

(a) $\alpha_m = 0°$

Figure 8.- Effect of airfoil thickness on lift derivatives.

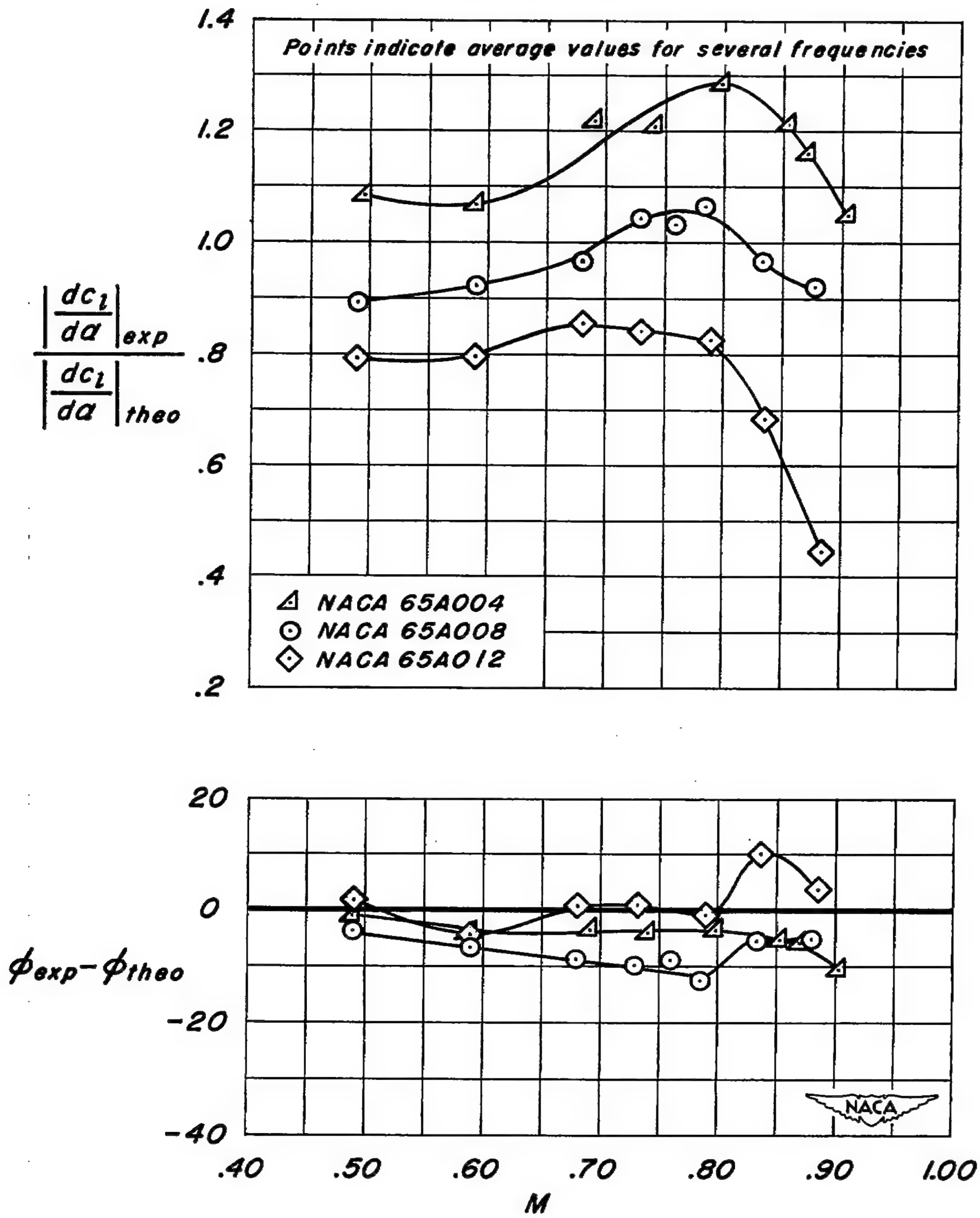

(b) $\alpha_m = 2°$

Figure 8.- Concluded.

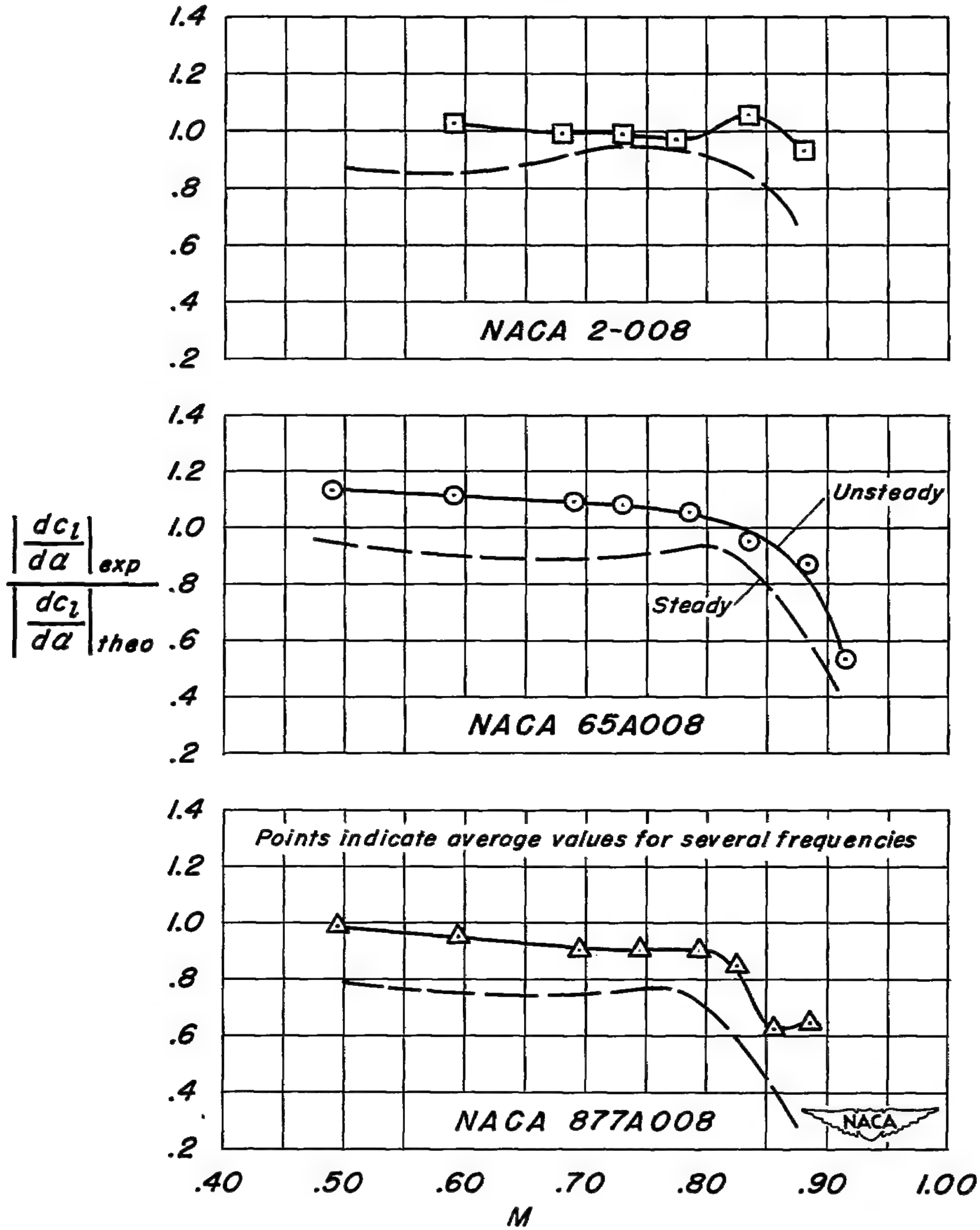

(a) $\alpha_m = 0°$

Figure 9.- Comparison of steady and unsteady lift derivatives for airfoils with varying thickness distributions.

[redacted]

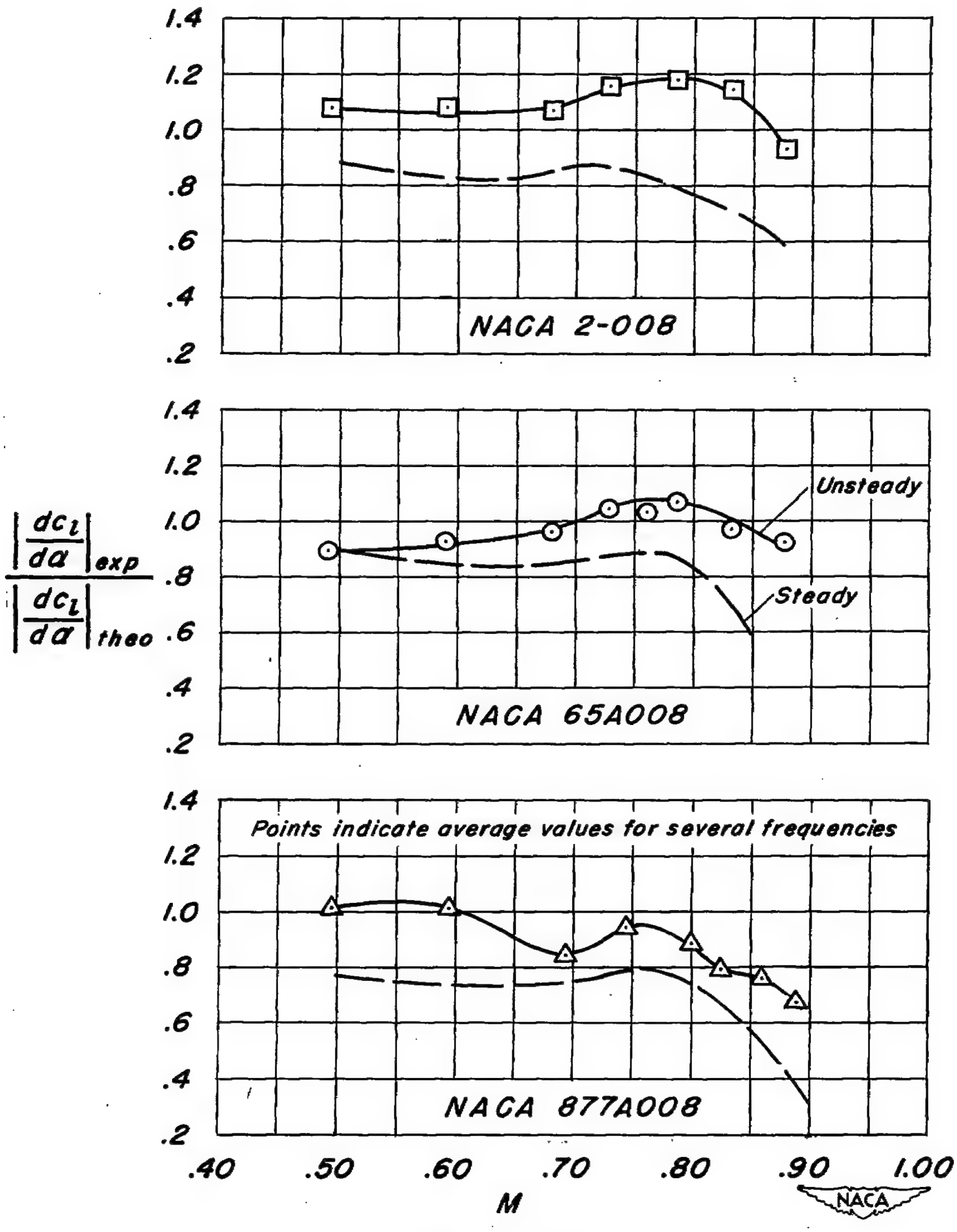

(b) $\alpha_m = 2°$

Figure 9.- Concluded.

[redacted]

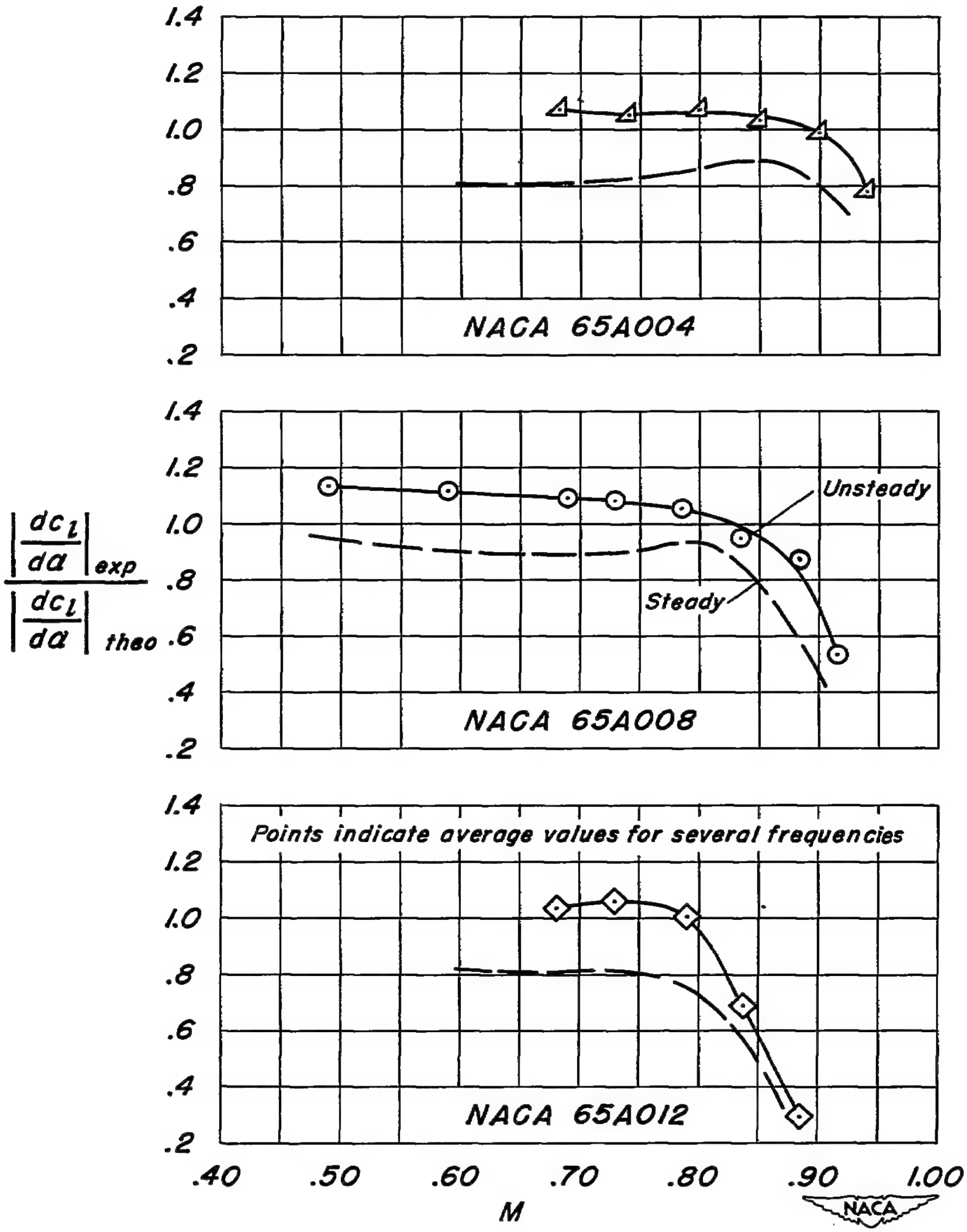

(a) $\alpha_m = 0°$

Figure 10.- Comparison of steady and unsteady lift derivatives for airfoils with varying thickness.

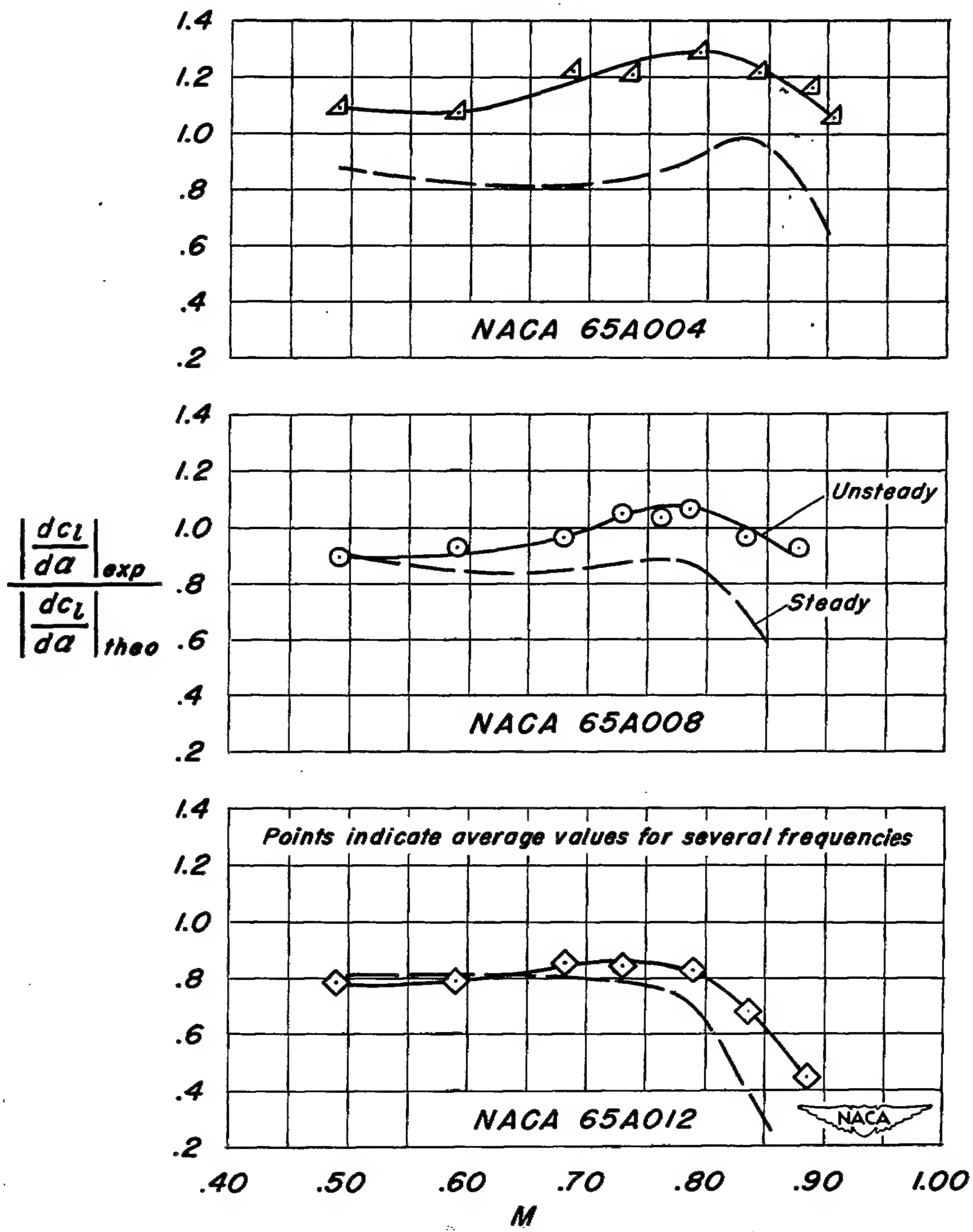

(b) $\alpha_m = 2^\circ$

Figure 10.- Concluded.

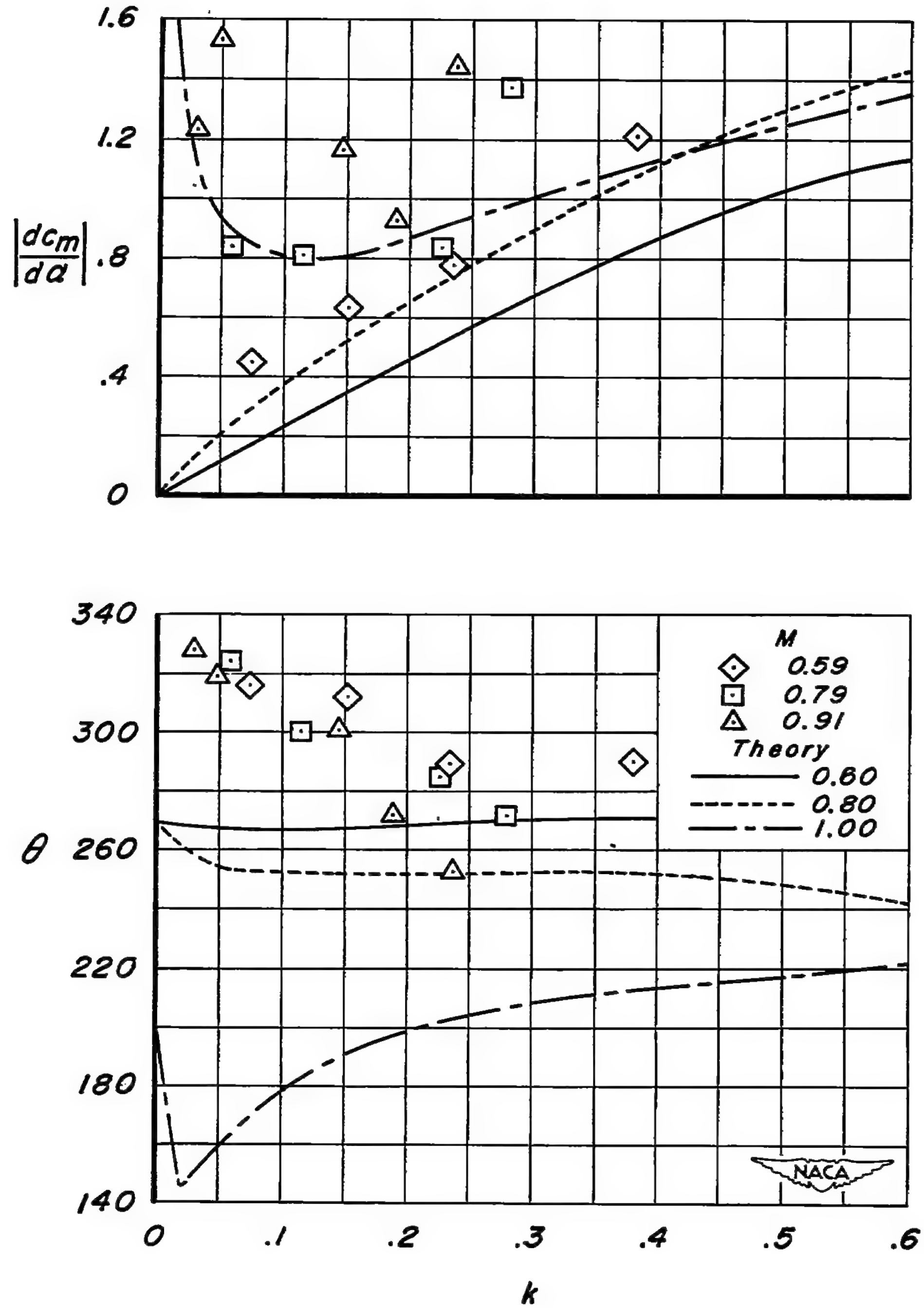

Figure 11.- Results as a function of reduced frequency, k, for several Mach numbers for the reference model, NACA 65A008; α_m = 0°.

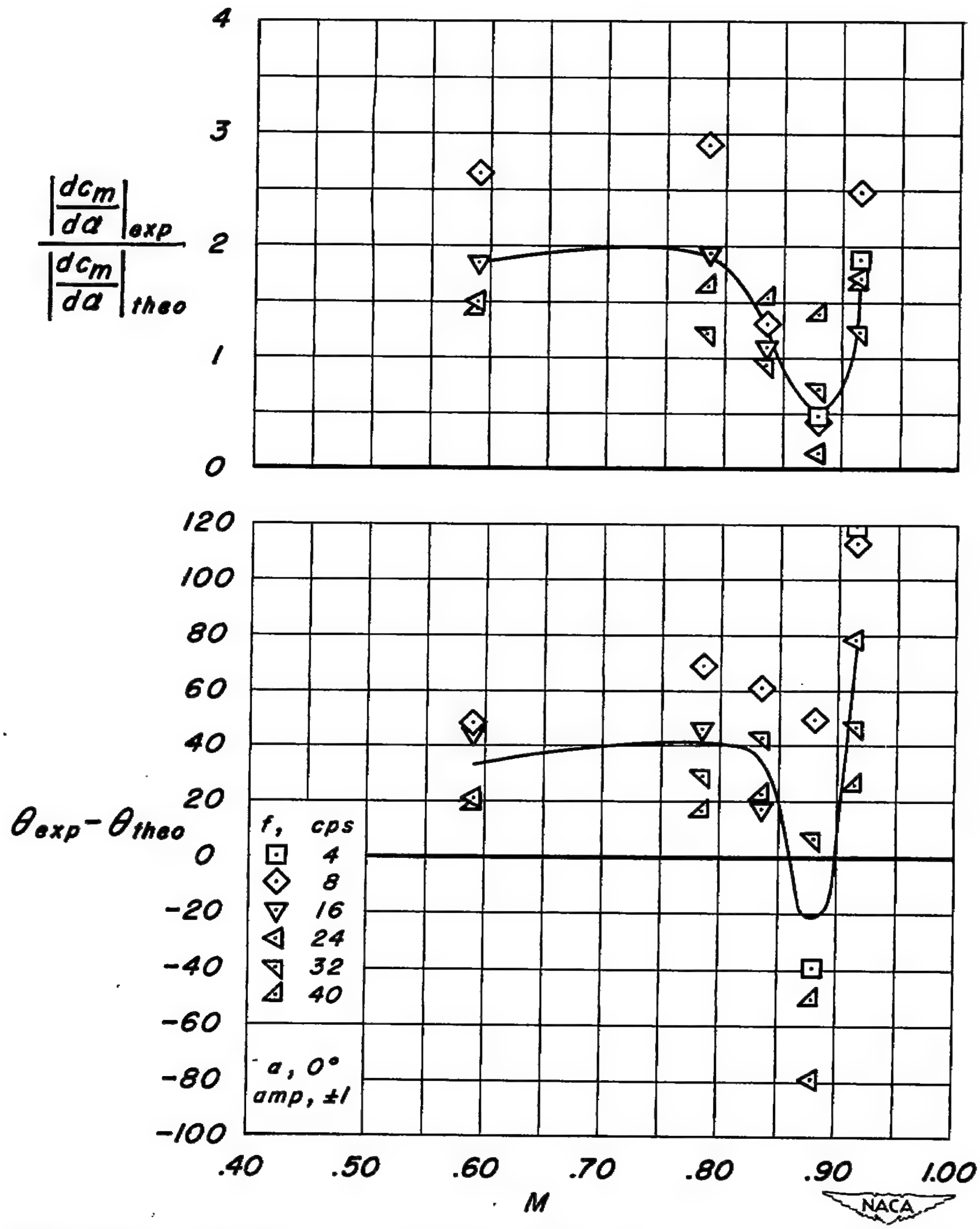

Figure 12.- Variation of experimental results from theory for reference model, NACA 65A008, with a faired line to show the mean variation with Mach number; $a_m = 0°$.

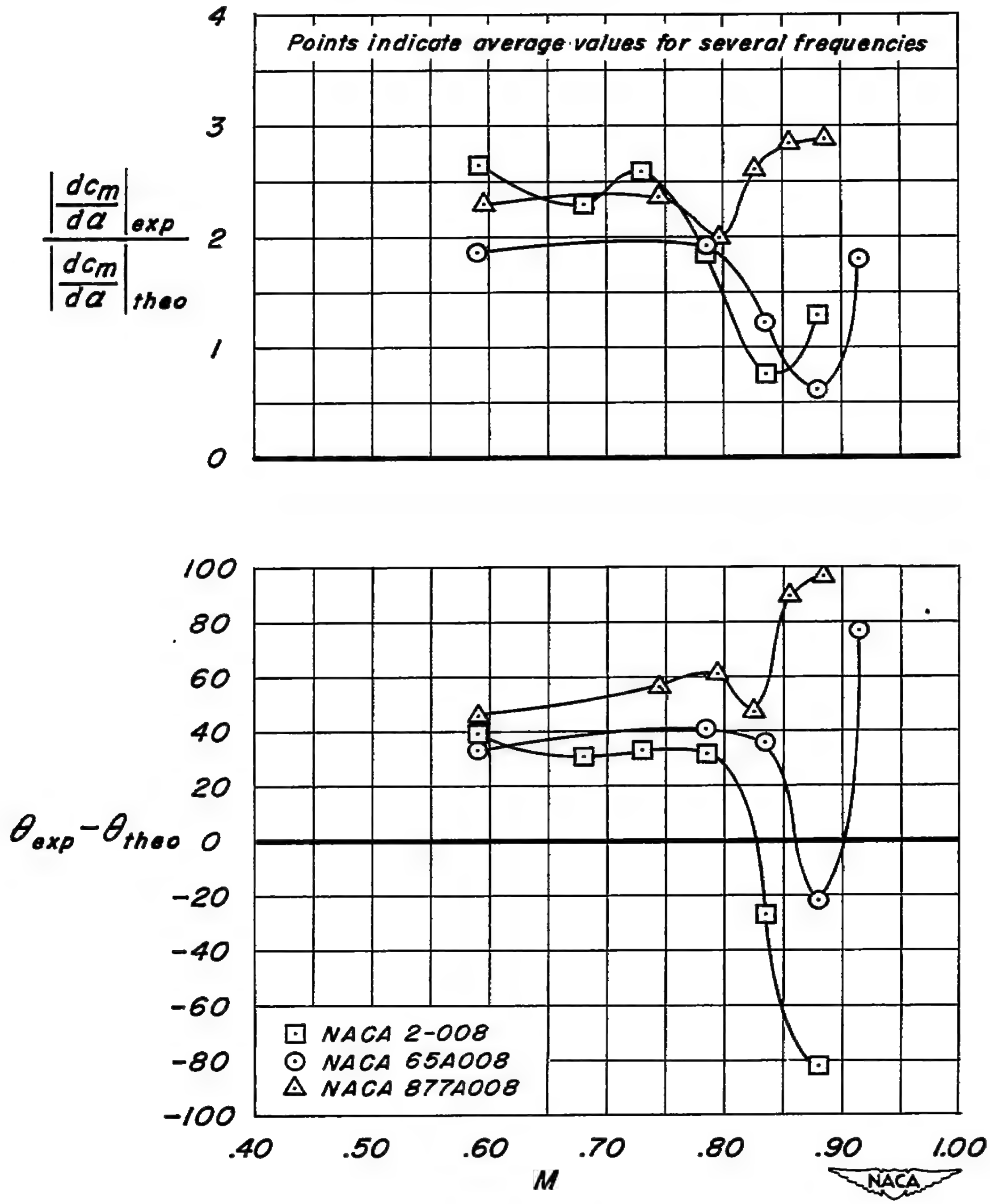

(a) $\alpha_m = 0°$

Figure 13.- Effect of airfoil thickness distribution on moment derivatives.

[redacted]

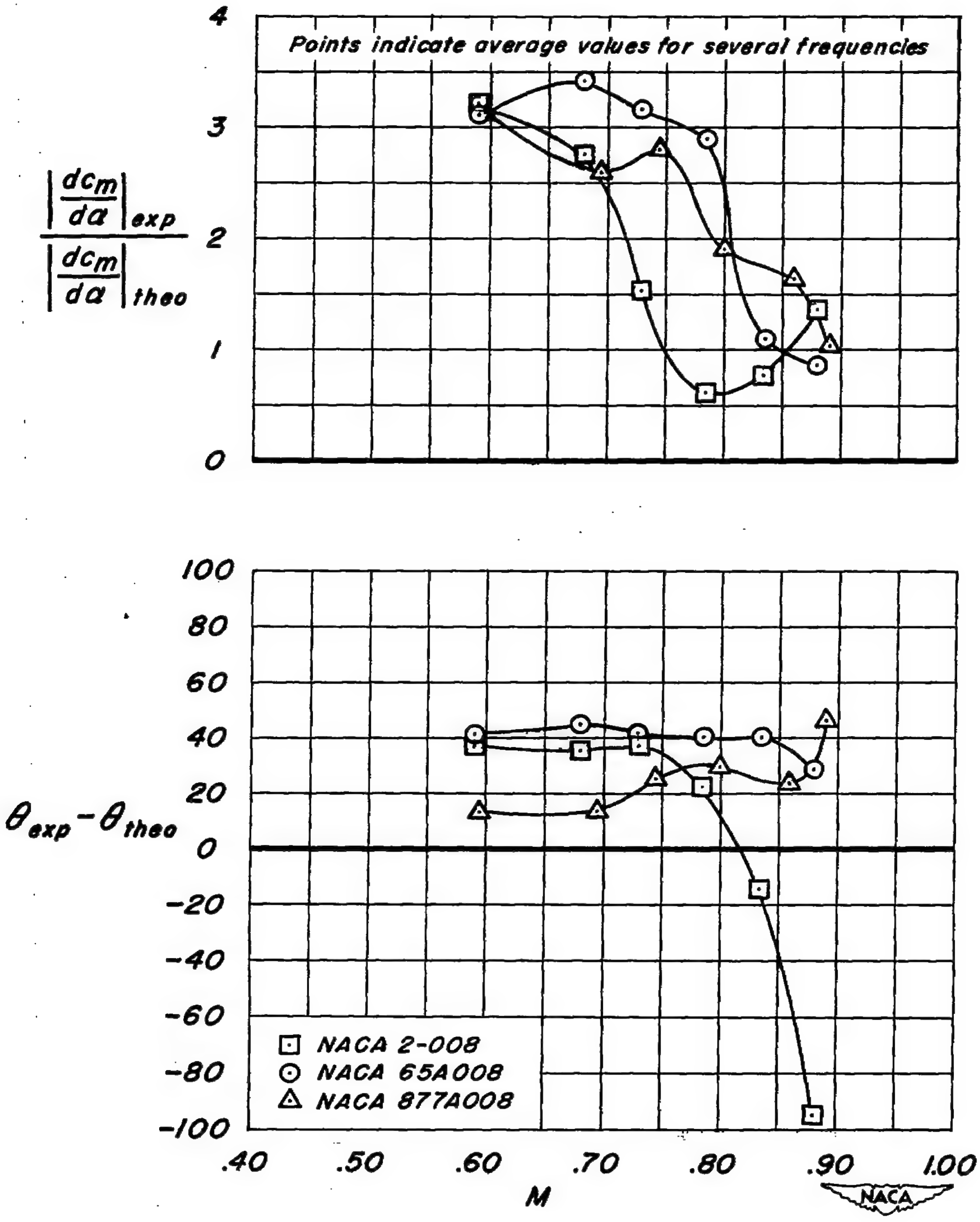

(b) $\alpha_m = 2°$

Figure 13.- Concluded.

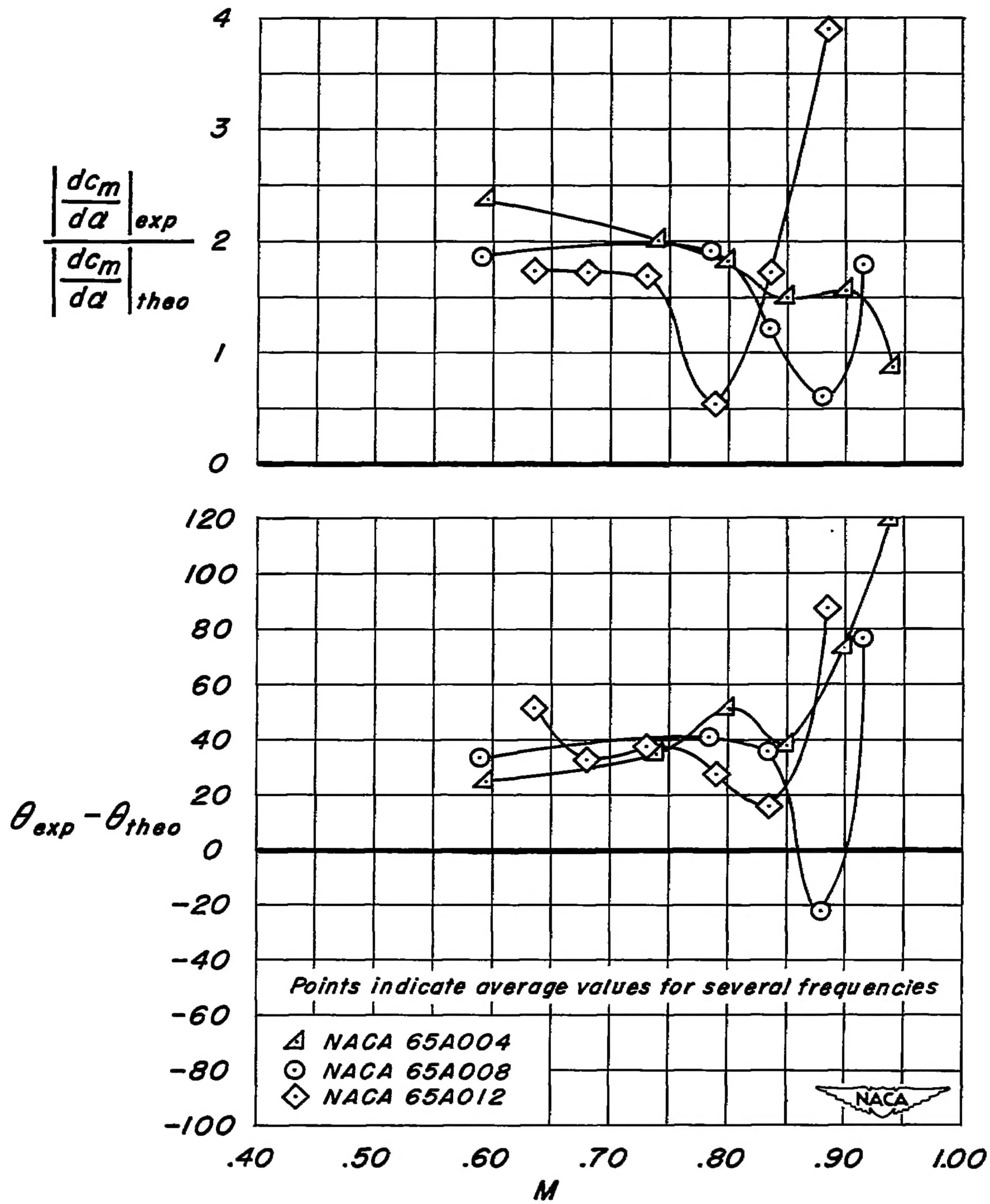

(a) $\alpha_m = 0°$

Figure 14.- Effect of airfoil thickness on moment derivatives.

[redacted]

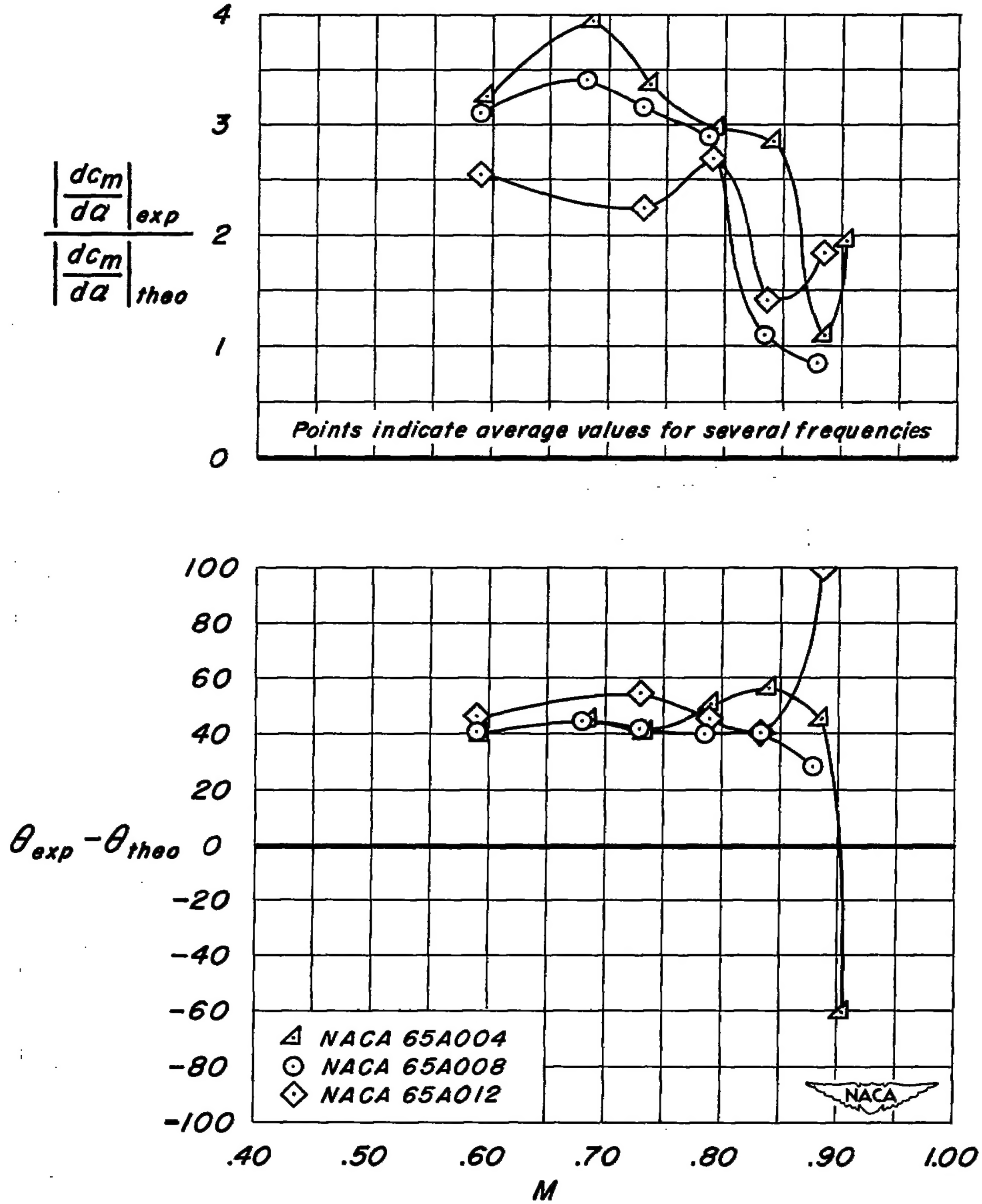

(b) $\alpha_m = 2°$

Figure 14.- Concluded.

[redacted]

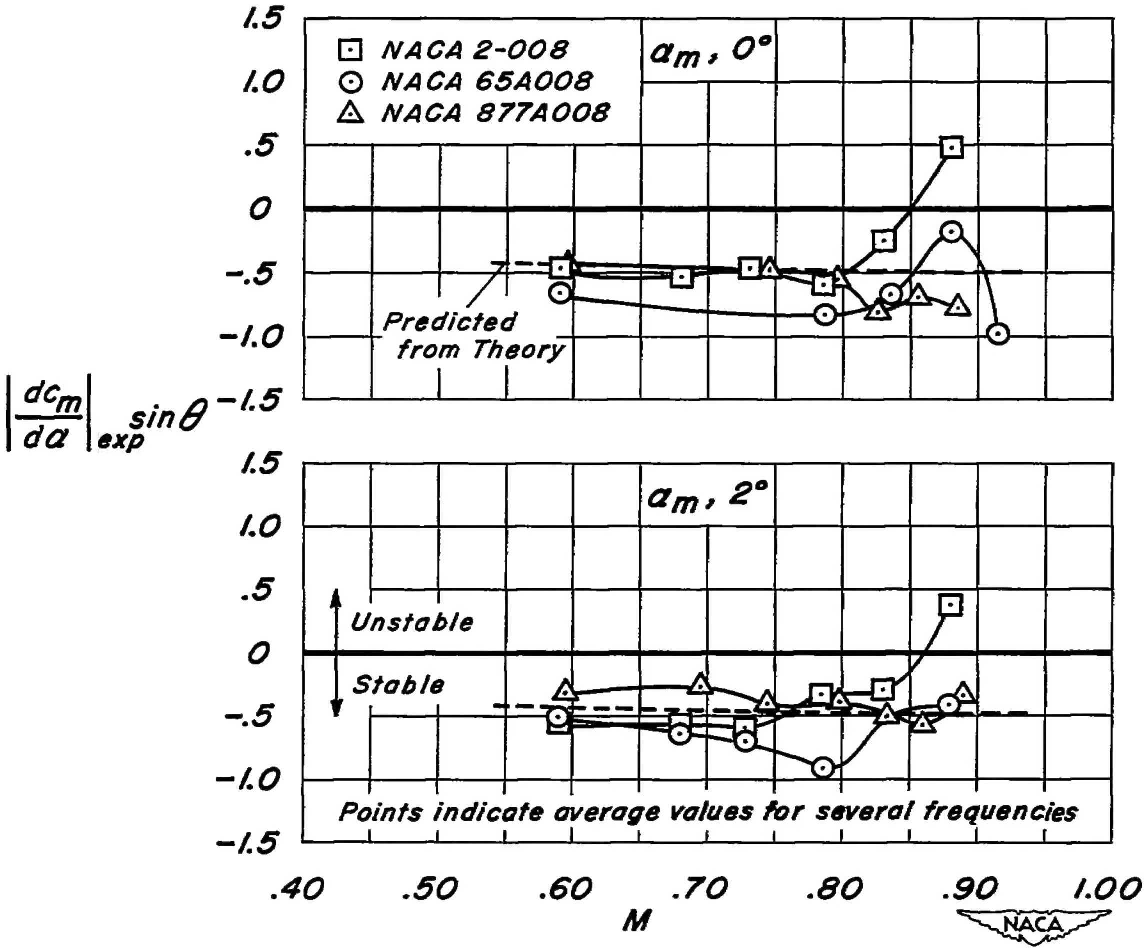

(a) Effect of airfoil thickness distribution.

Figure 15.– Damping component of the moment derivatives.

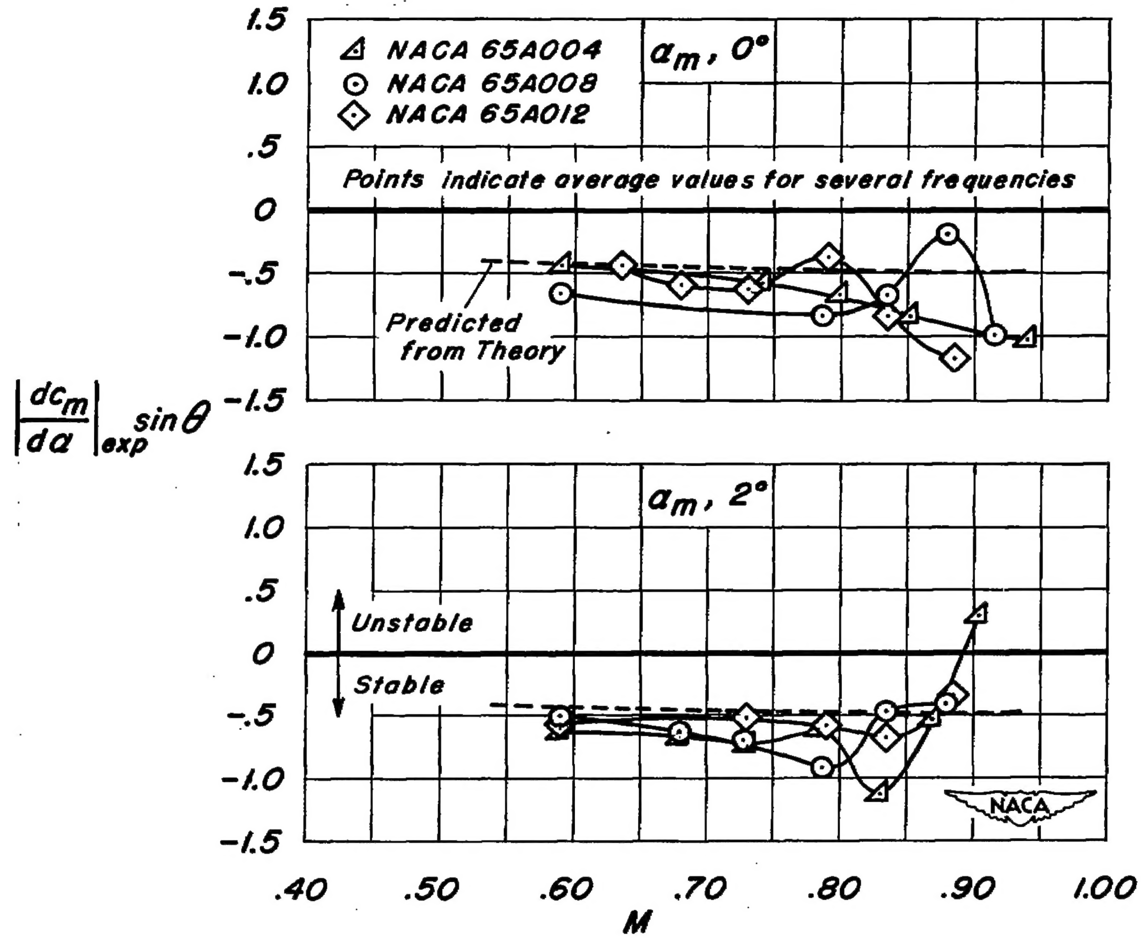

(b) Effect of airfoil thickness.
Figure 15.- Concluded.

[redacted]